

Mathematical Modeling of Laser Ablation

Bahador Vosooghi Chahar Oymaghi

Submitted to the
Institute of Graduate Studies and Research
in partial fulfillment of the requirements for the Degree of

Master of Science
in
Mechanical Engineering

Eastern Mediterranean University
June 2014
Gazimağusa, North Cyprus

Approval of the Institute of Graduate Studies and Research

Prof. Dr. Elvan Yılmaz
Director

I certify that this thesis satisfies the requirements as a thesis for the degree of Master of Science in Mechanical Engineering.

Prof. Dr. Uğur Atikol
Chair, Department of Mechanical Engineering

We certify that we have read this thesis and that in our opinion it is fully adequate in scope and quality as a thesis for the degree of Master of Science in Mechanical Engineering.

Prof. Dr. Hikmet Ş. Aybar
Supervisor

Examining Committee

1. Prof. Dr. Hikmet Ş. Aybar

2. Assoc. Prof. Dr. Hasan Hacışevki

3. Asst. Prof. Dr. Neriman Özada

ABSTRACT

In new surgery, there are various surgical methods for heating human tissue which are applied in an accurate and secure way. All these methods are based on particular applicator such as laser, radiofrequency device and microwave. In the past, Pennes defined bio-heat (BE) equation by considering Fourier's law of heat conduction to model heat transfer in biological tissues. With the progression of modern operational methods, medical therapies involve shorter time steps and higher heat fluxes, thus the classical model has been become inappropriate. The fact is that, the heat flux does not have enough time to propagate after imposing thermal energy. Therefore, this thesis introduces a more precise and pragmatic model by using of hyperbolic bio-heat equation (HBE) which uses thermal relaxation time τ that is necessary for heat propagation after radiation.

There are different types of numerical methods which are applied to analysis temperature distribution during laser heating. One of the frequently applied numerical methods is Finite Difference Method (FDM). In this study, FDM method is used for analyzing temperature profile for both standard and hyperbolic bio-heat equations in 7 different penetration depths. This analysis has been performed for two various initial temperatures 35°C and 40°C, the differences between two models for both initial temperatures have been reported and the effect of increasing initial temperature on the behaviors of two model has been investigated. To prove some specifications and benefits of the modified model, the results received from tissue heating with great energy fluxes are applied to correct Hyperopia (far-sightedness).

Keyword: Laser, heat transfer, biological tissues, bio-heat equation, cornea, modeling, Finite Difference Method.

ÖZ

İnsan dokusunu ısıtmak için, doğru ve güvenli bir şekilde uygulanan çeşitli yeni cerrahi yöntemler vardır. Tüm bu yöntemler, lazer, radyo frekans cihazı ve mikrodalga uygulayıcısı gibi belirli özel araçlara dayanmaktadır. Geçmişte, Pennes, biyolojik dokularda ki ısı transferini Modele Fourier ısı iletimi kanunu dikkate alınarak, bio-ısı (BE) denklemi tanımlamaktaydı. Modern işletme yöntemlerinin ilerlemesi ile, tıbbi tedaviler kısa zaman adımları ve yüksek ısı akısı içermektedir, böylece klasik modeli uygunsuz hale gelmiştir, Aslında ısı akışının termal enerjiyi heybetli sonra yaymak için yeterli zaman yoktur. Bu nedenle, bu tez radyasyondan sonra ısı yayılımı için gerekli olan termal gevşeme zamanı τ kullandığı hiperbolik biyo-ısı denklemini (HBE) kullanarak, daha kesin ve pragmatik modeli tanıtmaktadır.

Lazer ısıtması sırasında analiz ısı dağılımının uygulandığı sayısal yöntemlerin farklı türleri bulunmaktadır. Sık uygulanan sayısal yöntemlerden biri Sonlu Farklar Yöntemi (FDM) 'dir. Bu çalışmada, FDM yöntemi bir sıcaklık profili analiz etmek için 7 farklı penetrasyon derinliklerinde standart ve hiperbolik hem de biyo-ısı denklemleri için kullanılmaktadır. Bu analizin iki farklı başlangıç sıcaklıkları $35^{\circ}C$ ve $40^{\circ}C$ için yapılmıştır. İlk sıcaklıklar için iki model arasındaki farklar bildirilmiştir ve iki modelin davranışları üzerinde artan başlangıç sıcaklığına etkisi araştırılmıştır. Modifiye modelin bazı özellikleri ve faydalarını kanıtlamak için, büyük enerji akıları ile doku ısıtma da alınan sonuçları hipermetropta düzeltmek için uygulanmaktadır.

Anahtar Kelimeler: Lazer, ısı transferi, biyolojik dokular, biyo-ısı denklemi, kornea, modelleme, Sonlu Farklar Yöntemi.

To My Family

ACKNOWLEDGMENT

I would never have been able to finish my dissertation without the guidance of my committee members, help from friends, and support from my family.

I would like to express my deepest gratitude to my supervisor, Prof. Dr. Hikmet Ş. Aybar, for his excellent guidance, caring, patience, and providing me with an excellent atmosphere for doing research. I would like to thank my assistant Mehdi Moghadassi, who answer my entire question about research of laser ablation process in the field and practical issues beyond the textbooks, patiently corrected my writing and financially supported my research.

Finally, I would also like to thank my parents, two brothers, and older sister. They were always supporting me and encouraging me with their best wishes.

TABLE OF CONTENTS

ABSTRACT.....	iii
ÖZ	v
DEDICATION	vi
ACKNOWLEDGMENT.....	viii
LIST OF TABLES	xi
LIST OF FIGURES	xii
LIST OF SYMBOLS	xiv
1 INTRODUCTION	1
1.1 Laser Ablation of Biological Tissue.....	1
1.2 Laser Ablation in Human Eye	2
1.2.1 Cornea.....	3
1.2.2 Hyperopia and Myopia	6
1.2.3 Refractive Surgery	7
1.2.4 Laser Thermo-Keratoplasty	8
1.3 Aim of Study	9
1.4 Thesis Organization.....	11
2 LITERATURE REVIEW.....	12
2.1 Background of Laser Ablation in Biological Tissue	12
2.2 Parametric Survey of Laser Radiance Conditions on Ablation.....	15
2.3 History of Keratorefractive Procedures.....	15
3 MATHEMATICAL MODELLING.....	18
3.1 Parabolic and Hyperbolic Heat Transfer Models	18
3.2 Laser Heating	21

3.3 Numerical Method.....	25
3.3.1 Discretizing of PBE Model with Finite Difference Method.....	25
3.3.2 Cranks-Nicolson Method.....	26
3.3.3 Discretizing of HBE Model with Finite Difference Method.....	28
3.3.4 Discretizing of Boundary Condition.....	29
4 RESULTS AND DISCUSSIONS	30
4.1 Temperature Profiles for $T_0 = 35^\circ\text{C}$	31
4.2 Temperature Profiles for $T_0 = 40^\circ\text{C}$	35
5 CONCLUSION	41
REFERENCES.....	43
APPENDICES	51
Appendix A: Parabolic Bio-heat Equation.....	52
Appendix B: Hyperbolic Bioheat Equation.....	60

LIST OF TABLES

Table 1: Human cornea properties 30

LIST OF FIGURES

Figure 1: Schematic instance of laser ablation.....	2
Figure 2: Illustration of the eye structure.....	3
Figure 3: Illustration of cornea's layers.....	4
Figure 4: Cornea, red arrow: Descement's layer, blue arrow: Epithelium layer.....	5
Figure 5: Cornea: red arrow: epithelium, Blue arrow: Stroma.....	5
Figure 6: Illustration of hyperopia.....	6
Figure 7: Illustration of myopia.....	7
Figure 8: Schematic illustration of the geometric model for laser heating in human cornea. The laser light is perpendicular to the living tissue which has a semi-infinite shape ($x \geq 0$).....	21
Figure 9: Schematic irradiation process including absorption, reflection, scattering and transmission.....	22
Figure 10: Laser beam reduction as a function of penetration length.....	22
Figure 11: An illustration of the internal nodes for implicit method.....	26
Figure 12: Temperature profile for laser heating of the cornea at $x=0.01$ mm.....	31
Figure 13: Temperature profile for laser heating of the cornea at $x=0.05$ mm.....	32
Figure 14: Temperature profile for laser heating of the cornea at $x=0.1$ mm.....	32
Figure 15: Temperature profile for laser heating of the cornea at $x=0.3$ mm.....	33
Figure 16: Temperature profile for laser heating of the cornea at $x=0.5$ mm.....	33
Figure 17: Temperature profile for laser heating of the cornea at $x=0.7$ mm.....	34
Figure 18: Temperature profile for laser heating of the cornea at $x=1$ mm.....	34
Figure 19: Temperature profile for laser heating of the cornea at $x=0.01$ mm.....	36
Figure 20: Temperature profile for laser heating of the cornea at $x=0.05$ mm.....	36

Figure 21: Temperature profile for laser heating of the cornea at $x=0.1$ mm.....	37
Figure 22: Temperature profile for laser heating of the cornea at $x=0.3$ mm.....	37
Figure 23: Temperature profile for laser heating of the cornea at $x=0.5$ mm.....	38
Figure 24: Temperature profile for laser heating of the cornea at $x=0.7$ mm.....	38
Figure 25: Temperature profile for laser heating of the cornea at $x=1$ mm.....	39

LIST OF SYMBOLS

b	Absorption coefficient [1/m]
h	Convection coefficient [$W/m^2\text{°C}$]
I	Beam intensity [W/m^2]
k	Thermal conductivity [$W/m^2\text{°C}$]
L	Material length [m]
q	Heat flux [W/m^2]
R	Fresnel reflectance
S	Internal heat sources
T	Temperature [$^{\circ}\text{C}$]
x	Penetration depth [m]
Δt	Time step [s]
ΔT	Temperature difference [$^{\circ}\text{C}$]
Δx	Node distance [m]

Greek Symbols

α	Thermal diffusivity [m^2/s]
τ	Thermal relaxation time [s]
v	Heat propagation speed [m/s]

Abbreviations

FEM	Finite Element Method
HBE	Hyperbolic Bio-heat Equation

PBE	Parabolic Bio-heat Equation
PDE	Partial Differential Equations
YAG	Yttrium aluminum garnet

Chapter 1

INTRODUCTION

1.1 Laser Ablation of Biological Tissue

Laser ablation is an excellent technique for cutting and mass eliminating from biological tissue as a result of high deposited thermal energy in laser which has the ability to revolutionize a lot of surgical procedures (Fig.1). This device has three features:

- 1) The potential to produce short pulses of high intensity light.
- 2) The potential to precisely transfer this light to any place of the body.
- 3) The capability of removing or cutting one tissue kind over another selectively.

Empirical observations have illustrated that a singular laser pulse which has intensity from 10^5 to 10^9 W/m^2 can precisely eliminates a specific quantity of tissue with minimum damage to the surrounded area. Laser ablation has also the ability to apply in micro-surgery because laser beam can be delivered to a place even smaller than a micron and transmitted within fiber optical cables to almost any place of body. Furthermore, laser ablation is able to optionally influence one kind of tissue since leaving adjacent tissue [1].

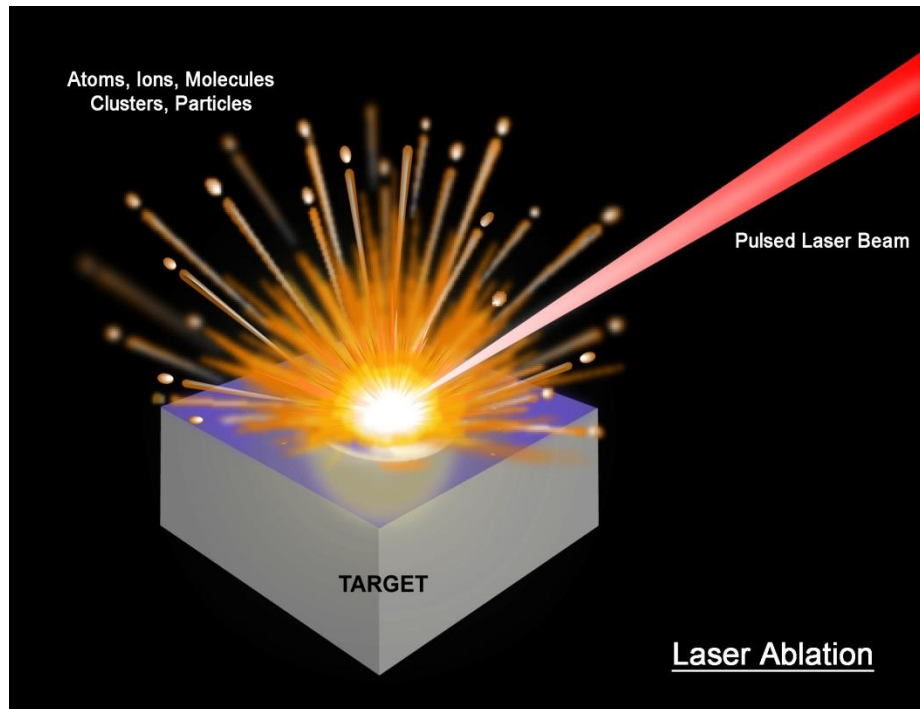


Figure 1: Schematic instance of laser ablation

1.2 Laser Ablation in Human Eye

Between different types of surgical procedures which employ laser heating, this study concentrates on corneal laser heating. For better understanding of this process, a brief explanation of the eye's structure is required. The cornea is a clear dome-shaped layer which is located in the center of external layer of the eye and makes up 1/6 of total size of this layer. The frontal chamber is between the iris and cornea which consists of aqueous humor that controls optical pressure [2]. The iris governs the quantity of the internal beams which meet the retina. The lens is situated at the back of the iris that is applied for adaptation [3]. Retina changes beam impulses into electrical signals and transfers them through the ocular nerve. At the end, this optical nerve sends the signals to the posterior lobe of the brain, which expounds these signals as optical images. Figure 2 shows various parts of eye [3].

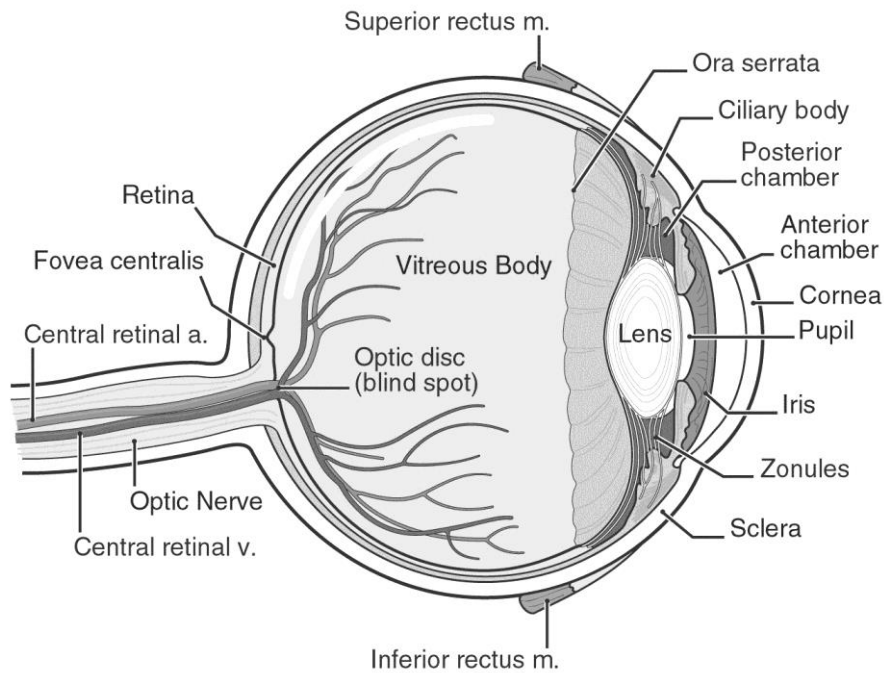


Figure 2: Illustration of the eye structure

1.2.1 Cornea

The cornea is a dome-shaped and clear window which covers frontal segment of the eye (Fig.2). The reason of clear and shiny surface is that there are not any blood vessels inside the cornea. Since, the cornea has the ability of supplying almost 2/3 of the eye's concentrating power; it is the most powerful refractive part of the eye which is in charge of converging internal light waves precisely. Basically, cornea includes collagen and 78% water [2].

Nowhere in the body has the amount of nerve endings as much as cornea which results in more sensitivity. As cornea is a vascular tissue, its reaction to illness processes is different from ones that have blood vessels.

The cornea of an adult with 0.56 mm thickness includes 5 various layers (Fig.2): epithelium, Bowman's membrane, stroma, Descemet's membrane and the endothelium.

- The epithelium is a Cellular layer which conceals the corneal surface. Its thickness is just 5-6 cell layers ($55\ \mu\text{m}$) which is $1/10$ of the overall thickness of the cornea and rapidly recreates when the cornea is hurt. However, the expansion of the injury results in losing the clarity of the cornea [4].

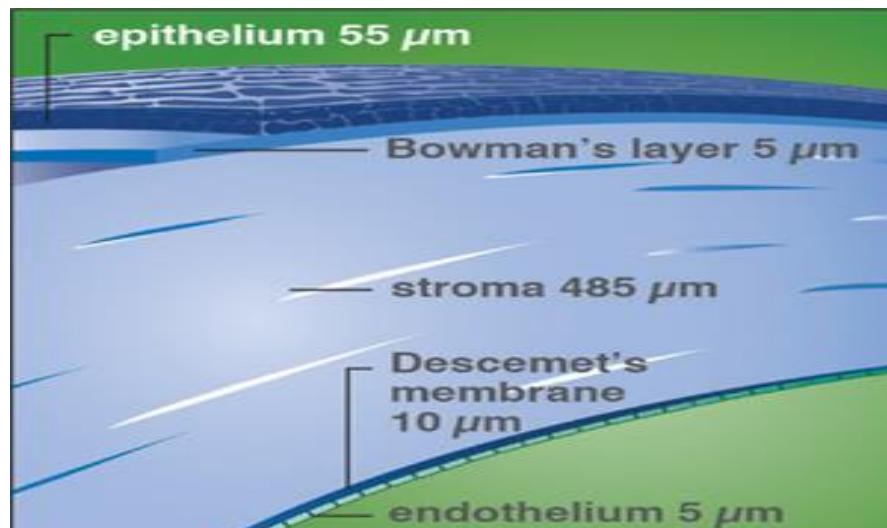


Figure 3: Illustration of cornea's layers [3]

- Bowman's membrane with $5\ \mu\text{m}$ thickness is under the epithelium layer (Fig.3) and supports the cornea from the damage because it is very hard to penetrate.
- The corneal stroma absolutely is a transparent connective tissue which is beneath Bowman layer and has the most thickness among other layers of the cornea with about $485\ \mu\text{m}$. The stroma usually includes 75% water. In addition, it is combined of compressed collagen fibers that move parallel to each other so that their particular structure leads to clarification of the cornea [3].

- Descemet's layer is below the corneal stroma and transfers water from the cornea and keeps it transparent. The thickness of this layer is near $10\ \mu\text{m}$ (Fig.4, 5) [3].
- The endothelium includes a singular layer of cuboidal that acts to hold the cornea dehydrated. Its width approximately is $5\ \mu\text{m}$. The endothelium temperature should not overtake 65°C to prevent thermal injury of the endothelium tissues [3].

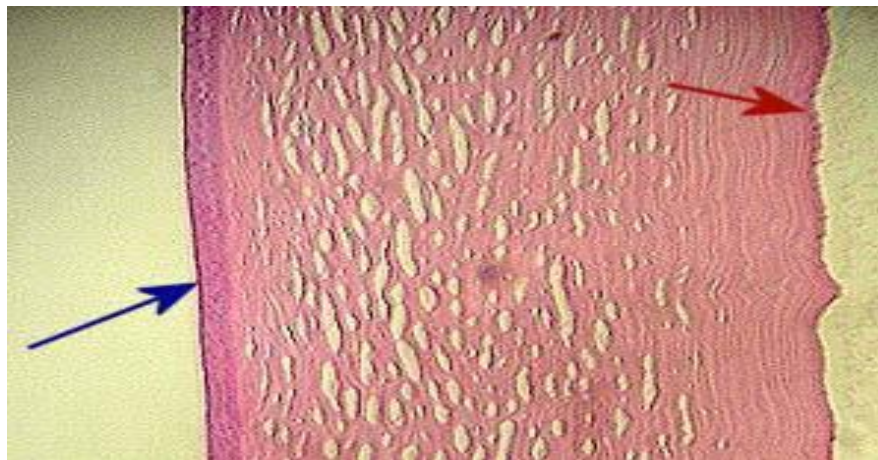


Figure 4: Cornea, red arrow: Descemet's layer, blue arrow: Epithelium layer [3]

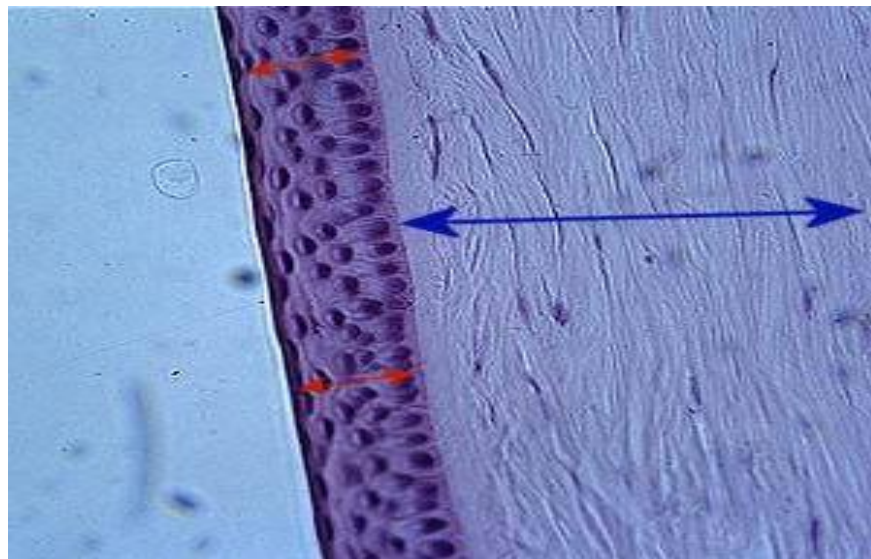


Figure 5: Cornea: red arrow: epithelium, Blue arrow:

1.2.2 Hyperopia and Myopia

Hyperopia or hypermetropia generally is known as farsightedness which is an imperfection of vision. This flaw happens for the ones who have too short eyeball or flat cornea. Therefore, their eyes don't have sufficient optic power to hold the lights in the center of the retina and they concentrate behind the retina [5]. These individuals cannot concentrate on targets at close distance very well and they often see blurred image of near objects (Fig.6) [6].

Myopia is opposite of the hyperopia which is commonly known as nearsightedness. In this case, incoming light focuses in front of the retina before reaching behind the cornea, causing the image that one sees when looking at a distant object to be out of focus, but in focus when looking at a close object (Fig.7) [7].

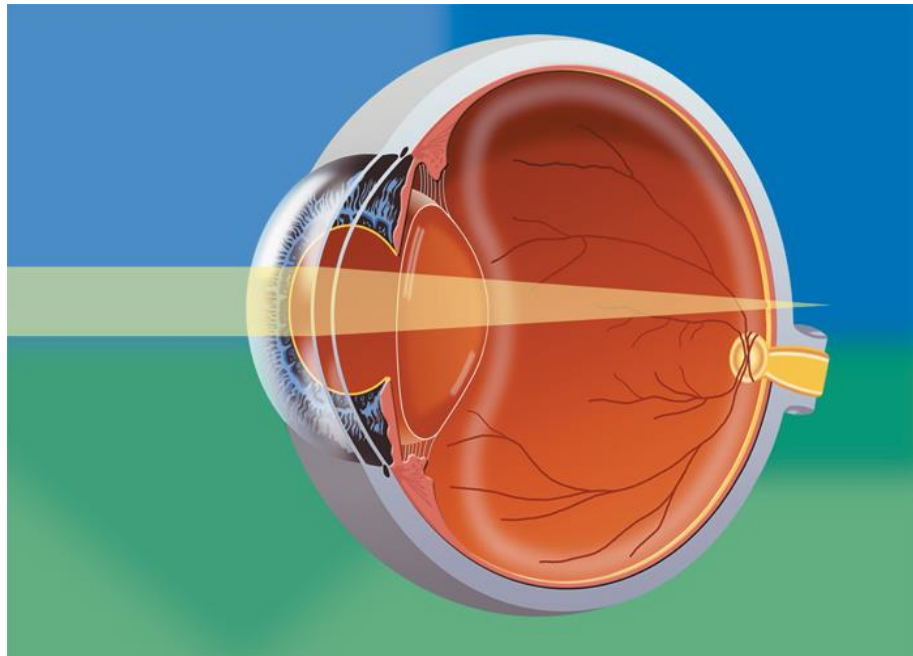


Figure 6: Illustration of hyperopia

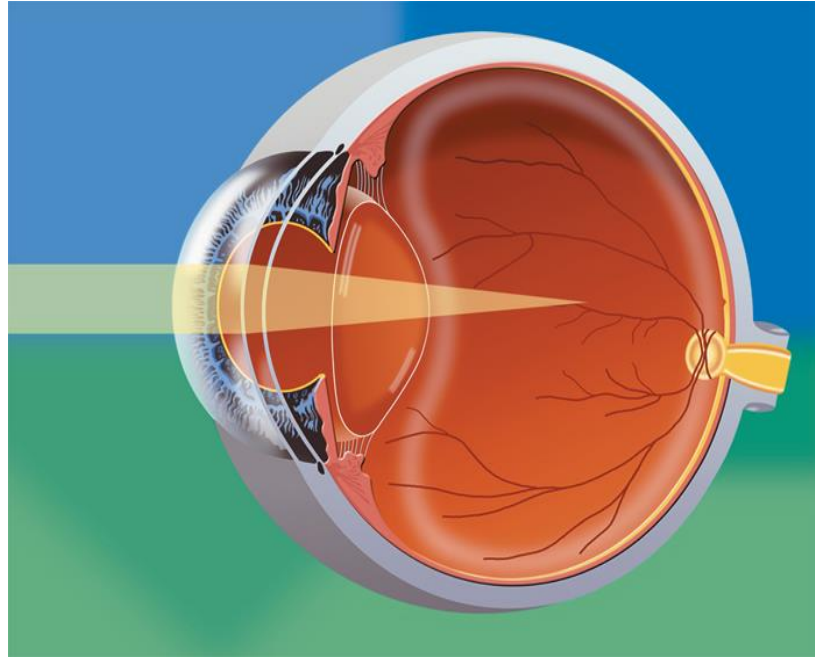


Figure 7: Illustration of myopia

1.2.3 Refractive Surgery

Traditionally, patients used to apply contact lenses and eyeglasses for vision correction which gave them inconvenience sense. Thanks to Lendeer Jans Lans (1896) research that illustrated the ability of refractive operation for the first time, affected people released from uncomfortable sensation. This technique applies to alter the corneal curvature which results in improving its refractive power. This improvement leads to producing a sharp picture upon retina. In its primary years, refractive technique was frequently realized to be risky and unstable [8]. With the advancement of treatment technology during the last 10 years, better results have been announced and the numbers of satisfied patients considerably increased [9-11].

Generally, there are two different groups of refractive surgery: keratorefractive, which the shape of the cornea is changed during operation; and intraocular, which combinatorial lenses are located inside the eye.

1.2.4 Laser Thermo-Keratoplasty

Among various kinds of keratorefractive surgical methods, this thesis focuses on laser thermo-keratoplasty (L-TKP). L-TKP is a non-excimer technique aimed to correct hyperopia by increasing the corneal curvature [12]. During L-TKP process the stromal collagen of the cornea is shrunk to a specific size by producing 8-16 laser points in a circular pattern at temperatures between 55°C and 65°C which results in increasing the corneal curvature while inducing lateral flattening [13]. In this method, medical tools and devices don't have physical contact with the cornea. The non-contact Holmium:Yttrium aluminum Garnet (Ho:YAG) lasers are typically applied in L-TKP process which heats the cornea in the middle infrared area with wavelength 2.1 μm [13].

Although L-TKP have successfully been used in the past that is not a suitable technique for clinical therapy of hyperopia in comparison with photo-refractive keratectomy because L-TKP has low ability of duplication and prediction in producing valid outcomes. Nonetheless, L-TKP is yet a famous technique for treatment of hyperopia.

Over the last years, various explorations have been performed to survey the thermo-mechanic treatments of the cornea during L-TKP to better its ability of duplication and prediction. At primary experiments, researchers preferably made using of the animal's eye as a test specimen to prevent probable thermal injury of L-TKP to the human cornea. These samples were also good choices for mathematical explorations because of their facility of implementation. By development of advanced computational system, more accurate and realistic models could be achieved to better precision of the simulated solution [14].

For easement of these investigations, multitude models presumed extremely simplified geometries and primary-boundary conditions to investigate temperature propagation through the cornea [14]. Mainster et al [15] and Peppers et al [16] modeled laser heating of the cornea in one-dimension with considering the tissue as a half-plane. Subsequently, absorbed laser energy by the cornea was modeled by Beer-Lambert's law. Mainster et al and Zhou et al [17-20] used a finite cylindrical model to compute temperature diffusion of the cornea during L-TKP. Unlike the last models, Brinkmann et al modeled the behavior of laser light inside the cornea by measuring of light tracing in order to study corneal thermal reaction under different situation within L-TKP [21-23].

Lately, Podol'stev and Zheltov [24] applied multi-layered cylindrical model to survey heat transfer in the cornea within L-TKP. In this process, the irradiated laser light at the middle of the sample was supposed to be scratched and absorbed inside any area of the eye and the outcomes were used to recognize the threshold situations for corneal photo-destruction.

1.3 Aim of Study

The goal of this thesis is to model heat transfer occurs during the laser heating of the human cornea. Traditionally, modeling of heat transfer is performed by applying parabolic bioheat equation (PBE) which considers Fourier's law of heat transfer. Nevertheless, it is demonstrated that on very short scales of time this model is not reliable enough. Because heat flux (effect) and the temperature gradient (cause) happen at the same time (t) hence thermal energy is propagated with infinite speed over the target zone. An improved version of PBE model is presented by applying

hyperbolic bioheat equation (HBE) with finite heat diffusion speed. This model uses thermal relaxation time τ which is necessary for heat propagation after radiation.

With progression of computers in engineering fields, various researchers applied the new computational procedures to model temperature distribution during the heating of the cornea. One of the frequently applied methods is Finite Difference Method (FDM). This numerical method works through dividing complicated geometry into small volume in order to change Partial Differential Equations (PDE) to an easier linear geometry. FDM gives a proximate outcome since it uses calculus variation procedures and reduces the errors by repetition. This procedure specifically uses to solve PDEs that are unsolvable by analytical procedures in complicated geometry. In this study, FDM method is used for analyzing temperature distribution for both PBE and HBE models in seven different penetration depths. This analysis has been performed for two various initial temperatures 35°C and 40°C. The differences between two models for both initial temperatures have been reported and the effect of increasing initial temperature on the behaviors of two models has been investigated. The FORTRAN programming language is used in order to solve related equations. The considered assumptions for this study are:

- 1) Transient form of energy equation will be solved.
- 2) One-dimensional ablation will be considered.
- 3) The properties of the cornea will be assumed constant during laser heating process.
- 4) Lateral heat transfer in other parts will be assumed negligible.
- 5) The properties of the cornea will be supposed isotropic.

1.4 Thesis Organization

This study has been organized in 5 Chapters:

In Chapter 1, a brief introduction about laser ablation of biological tissue has been expressed. Structure of the human eye and the layers of the cornea are explained. At the end, laser heating of the human cornea which is applied for vision correction has been described.

In Chapter 2, a short background of various applications of laser ablation in medicine is explained. Different experimental works which evaluate the effects of some parameters on ablation rates have been expressed.

Chapter 3 tries to compare parabolic bio-heat equation (PBE) with infinite heat propagation speed and a more accurate model of PBE with finite speed which is known as hyperbolic bio-heat equation (HBE). For mathematical modeling, partial derivatives $\left(\frac{\partial T}{\partial t}, \frac{\partial^2 T}{\partial x^2} \text{ and } \frac{\partial^2 T}{\partial t^2} \right)$ have been discretized separately by using of Crank-Nicolson method and they are substituted in final form of PBE and HBE models.

In the Chapter 4, the results of modeling are illustrated in the various diagrams and the differences between two models are defined in details.

In the Chapter 5, conclusion of study is reported

Chapter 2

LITERATURE REVIEW

2.1 Background of Laser Ablation in Biological Tissue

Nowadays, laser ablation with short pulses is widely applied and developed in many various medical applications such as ophthalmology, cardiology, otolaryngology, dermatology, orthopedic, dentistry, urology and gynecology.

As a matter of fact, hypothesis and physical experiments led to advancement of all existing medical laser devices. Einstein (1917) was the first person who defined that speeded up electrons generate electromagnetic lights in a specified wavelength and he anticipated the existence of simulated transpiration of radiation. After about four decades, Theodore Harolf Maiman (1960) invented the first ruby laser (wavelength=694.3 nm) that was made with respect to the concept of optical maser (a device that generates continued electromagnetic wave). Following this, Brech and Cross (1962) evaluated the spectrum of the shiny plasma which was produced by ruby laser. This research fundamentally was organized for the elemental resolution of a solid substance by laser microprobe transpiration spectroscopy [25]. Campbell et al (1963) announced the first ruby laser application in medicine for treating retinal tears. For this purpose, they combined xenon photo-coagulation and ruby laser in order to repair the primary retinal detachment options [1].

Schenk et al (1990) investigated toward using of the laser to operate the bone of the mid ear to better hearing. As it is aimed, they applied three various lasers (Alexandrite, Erbium:YAG, Ho:YAG) to ream a hole into the incus during microscopic process for fixing ear prosthesis [1].

In dermatology, Bohigian et al (1988) announced a method which is applied to treat patients who were being infected with Rhinophyma (gross and ruddy nose) by using of CO_2 laser. This laser provides a great visualization in order to operate a precise cutting of the glands [26].

Kaufman and Hibst (1989) used pulsed Er:YAG laser (with 2,945 nm wavelength) to eliminate surface epidermal sores with low amount of thermal damage to adjacent region [27]. Since Er:YAG irradiance is strongly absorbed by tissue water ($\mu \sim 1,000 \text{ mm}^{-1}$); the tissue (more profound than $\sim 5 \text{ mm}$) under the human skin surface is heated by heat propagation from the surface layer [28].

Declining the rate of heart attacks is one of the laser ablation's usages which is known as laser angioplasty. In this method, laser removes atherosclerotic plaque through the coronary blood vessels. Despite the fact that this method has enormous potential, some crucial problems are yet under exploration. Deckelbaum (1996) reviewed the results of investigations. He defined that elimination of plaque substance can cure untreatable wounds and decline restenosis rates since energy of laser can evaporate atherosclerotic plaque [29]. Earlier studies about ablation process of atherosclerotic plaque were carried out [30].

There is a possible application of laser ablation in dentistry where the corrosion of glaze and dentine is being researched for feasible application in dental methods [31]. In this procedure, the pulsed Er:YAG ($\lambda = 2.94 \mu\text{m}$) laser has been used to ablate dental strong tissue and ablation efficiency was measured by evaluation of mass elimination rate [32].

In orthopedic, treatment of intervertebral discs sicknesses by subcutaneous laser discectomy method is being extended [33]. In this operation, a special surgical instrument which is called curettes is applied to scrap the disk under endoscopy device. Little osteophytes (bony curvatures which form in joint margins) are removed by applying micro-curettes, and afterwards Ho:YAG laser (500 J, 8.5 W, 10 Hz, 5 seconds on/5 seconds off) is applied to eliminate disc substance (laser thermal disko-plasty) [34, 35].

In urology, Neodymium-doped: YAG (Nd:YAG) laser is being applied to ablate groups of surface urinary bladder cancer. Contrary to the electrosurgical elimination which needs anesthesia; this operation is performed on an outpatient situation and does not need anesthesia [36].

Laser lithotripsy is an operation applying Ho:YAG laser (350 μs pulse duration and 10 HZ pulse rate) to segment gallstones into tiny parts where they can be simply excreted [37].

The application of fiber optic which was produced by pulsed laser beams is being examined to cure endometriosis in the gynecology section [38].

2.2 Parametric Survey of Laser Radiance Conditions on Ablation

Many scientists have performed various empirical works about the effect of intensity, wavelength and its fluence in the ablation of human tissue (whether soft or hard). The interplay between laser and tissue primarily is controlled by the beam absorption through the tissue. Since these absorption features of tissue are extremely related to wavelength, a suitable choice of wavelength leads to a great selectivity. Depending on types of tissues, a variety types of laser such as XeCl excimer laser ($\lambda=308$ nm), flash-pumped color laser ($\lambda=295-590$ nm), Nd: YAG laser ($\lambda=355$ nm), Alexandrite laser ($\lambda=375$ nm) and Hydrogen fluoride laser ($\lambda=2.7-2.9$ μm) were applied. The range of pulse duration was between 7.5 ns and 250 μs . During different experiments, scientists studied interaction between laser and tissue by radiating the target instance in several laser pulses at a specific wavelength and fluence. They applied powerful microscopes to specify the influence of laser radiance on biological tissue. The outcomes of these experimental works provided some significant information about ablation process. For instance they could define a fluence threshold for laser ablation process. For fluencies under threshold, radiation did not have visible influence on the target sample [39].

2.3 History of Keratorefractive Procedures

Hyperopia and myopia correction by refractive methods has a long background. Leendert Jan Lans (1896) announced the first original exploration of keratoromy and explained the principles of it. Subsequently, he defined a procedure to correct astigmatism by reshaping the cornea. The Lans award, which is the most famous award of the international association of refractive surgery of ophthalmology, is named after him because of his attempts to ophthalmology [40].

Another famous award of this association is named after José Ignasi Barraquer (1949) who expanded the rules of lamellar surgery which consists of elimination of the corneal collagen. In the 1960's, he investigated keratomileusis method which is applied for correcting myopia that encountered cutting a button of stromal collagen with a microkeratome, shrinking it and inserting it in the human's cornea. However, this method did not have a good control on refractive results [41].

Trokel et al (1983) recommended the application of the excimer laser (193nm) as an accurate technique to change the corneal curvature. The first use of this type of laser was Photorefractive Keratectomy which was applied to correct myopia. He used excimer laser to remove epithelium and then stromal collagen of the cornea under computer monitoring which led to increasing refractive power of the cornea [41].

During 1980s, Svyatoslav Fyodorov expanded hyperopic thermokeratoplasty applying a warmth nickel-chromium probe which was able to penetrate up to 90% of corneal thickness by producing thermal burns to 600°C [42].

The failure of hot wire method to provide a permanent, predictable and secure hyperopia correction resulted in exploration of other methods of thermal keratoplasty. Theo Seiler (1990) made the first prosperous use of contact Ho:YAG laser to correct hyperopia. Van Saarloos and Constable (1993) applied Ho:YAG lasers (wavelength of 1500-2200 nm) in order to shrink collagen of the cornea down to a specified size for correcting near-sightedness in an accurate way [43]. During laser heating of the cornea 8-16 laser points were applied in a circular pattern at temperatures between 55 °C and 65°C which led to increasing the corneal curvature [13].

Over the last decades, many scientists, research laboratories and companies have endeavored to find and develop new applications of laser ablation in medicine however many fundamental levels of laser application are largely still unexplored.

Chapter 3

MATHEMATICAL MODELLING

3.1 Parabolic and Hyperbolic Heat Transfer Models

Heat transfer among biological tissue is a very complex process since it involves several processes such as conduction, blood perfusion, convection and metabolic activity. Over the last decades, heat transfer has been modeled by different mathematical equations. The most valid equation applying for this purpose is the heat conservation equation with interior source $S(x, t)$:

$$\nabla \cdot q(x, t) + \frac{k}{\alpha} \frac{\partial T}{\partial t}(x, t) = S(x, t) \quad (3.1)$$

Where q , T , k and α denote the heat flux, the temperature, thermal conductivity and thermal diffusivity $\left(\alpha = \frac{k}{\rho c}\right)$ (ρ being density and c specific heat) respectively.

According to Fourier's law, $q(x, t)$ is proportional to the minus of temperature gradient as:

$$q(x, t) = -k\nabla T(x, t) = -k \frac{\partial T}{\partial x}(x, t) \quad (3.2)$$

Pennes (1948) introduced the standard bio-heat equation (BE) by substituting Eq.3.2 into the Eq.3.1 to model temperature distribution during the heating of human tissue by considering $S(x, t)$ as heat sources [44]:

$$-\frac{\partial^2 T}{\partial x^2}(x, t) + \frac{1}{\alpha} \frac{\partial T}{\partial t}(x, t) = \frac{1}{k} S(x, t) \quad (3.3)$$

This equation is also known as parabolic bio-heat equation (PBE) which supposes an infinite speed for thermal propagation. In other words, each local temperature perturbation results in an instant temperature disturbance at every point of the tissue.

When this equation is applied to study thermal treatments, the interior heat sources $S(x, t)$ usually include three various sources:

$$S(x, t) = S_s(x, t) + S_p(x, t) + S_m(x, t) \quad (3.4)$$

Here, $S_s(x, t)$, $S_p(x, t)$ and $S_m(x, t)$ are surgical thermal energy source, blood perfusion and metabolic activity source respectively. Since second and third terms do not have effect on the laser heating process, they are assumed negligible and $S(x, t)$ just have been shared from surgical source $S_s(x, t)$.

With the progression of modern surgical method, therapies involve shorter time steps and higher heat fluxes, thus the standard BE with infinite heat propagation speed will fail because on short time scales $t \in [0, \tau]$, with adequately short amount for $\tau > 0$, heat flux does not have enough time for propagation after imposing laser light hence thermal balance of a developed physical system easily cannot be provided.

For this purpose, Cattaneo and Vernotte introduced an improved form of Fourier's law which applies thermal relaxation time τ for the laser heating process. This equation therefor is formulated by applying the simplest generalization for finite heat diffusion speed as:

$$q(x, t + \tau) = -k \frac{\partial T}{\partial x}(x, t) \quad (3.5)$$

In this equation heat flux (effect) and the temperature gradient (cause) happen at various time $t+\tau$ and t respectively and τ is a necessary time for propagation of the heat flux after imposing temperature gradient. Eq.3.5 demonstrates that the heat flux, depending on τ , does not initiate immediately, but increases gradually after applying the temperature gradient [45]. For small relaxation time τ Eq.3.5 is expressed as:

$$q(x, t) + \tau \frac{\partial q}{\partial t}(x, t) = -k \frac{\partial T}{\partial x}(x, t) \quad (3.6)$$

By combining Eq.3.6 with Eq.3.1, one directly gains the hyperbolic bio-heat equation (HBE) with a wave term (double-derivative term) and interior heat sources [46]:

$$-\frac{\partial^2 T}{\partial x^2}(x, t) + \frac{1}{\alpha} \left(\frac{\partial T}{\partial t}(x, t) + \tau \frac{\partial^2 T}{\partial x^2} \right) = \frac{1}{k} \left(S(x, t) + \frac{\partial S}{\partial t}(x, t) \right) \quad (3.7)$$

For $\tau = 0$, HBE model changes into the standard Fourier model. Wave term (double-derivative term) with $\tau > 0$ is one special specification of Eq.3.7 which increases wave properties and it represents finite heat propagation speeds that is formulated as:

$$v = \sqrt{\frac{\alpha}{\tau}} \quad (3.8)$$

3.2 Laser Heating

In this thesis, the concentration is on optic laser heating or laser thermokeratoplasty (L-TKP). During this process, a semi-infinite piece of isotropic living tissue is assumed so that laser light radiates to the whole surface of the tissue. As Figure 8 illustrates, laser heating occurs in one-dimension and the direction of radiation is parallel with the axis of chosen geometric model (x -axis). At top of the surface ($x < 0$), free thermal convection is assumed for cooling the corneal surface.

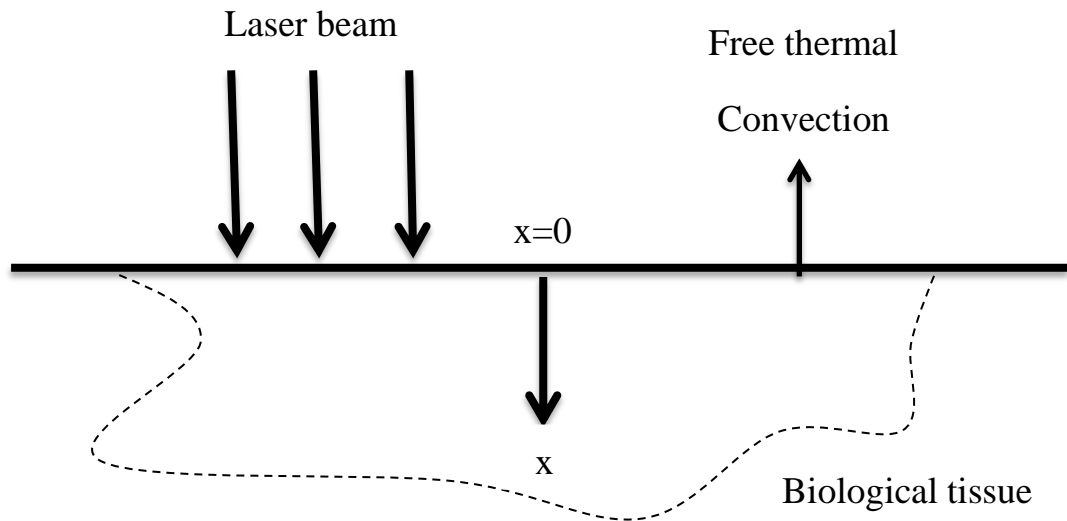


Figure 8: Schematic illustration of the geometric model for laser heating in human cornea. The laser light is used perpendicular to the living tissue which has a semi-infinite shape ($x \geq 0$) [44].

When a laser light irradiates tissue surface, one part of the light reflects and the rest absorbs into the surface. This absorbed beam attenuates basically in the two various ways: scattering and transmission (Fig.9). Generally, the cornea attracts approximately 95 % of the laser light during laser heat and a little part of beam (5%) reflects from the tissue surface and the transmission of laser light to other places of the human eye is considered negligible during radiation.

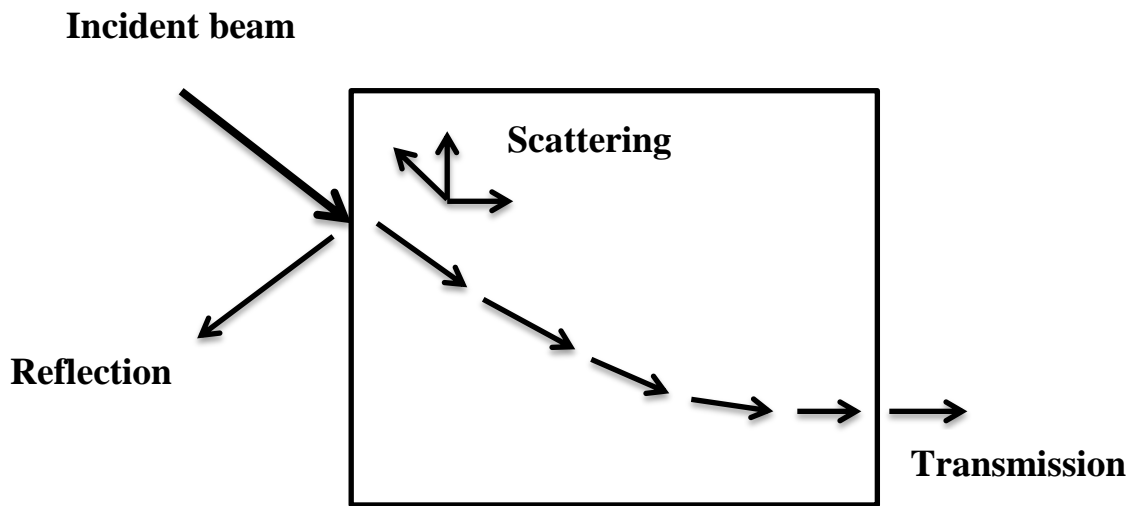


Figure 9: Schematic irradiation process including absorption, reflection, scattering and transmission

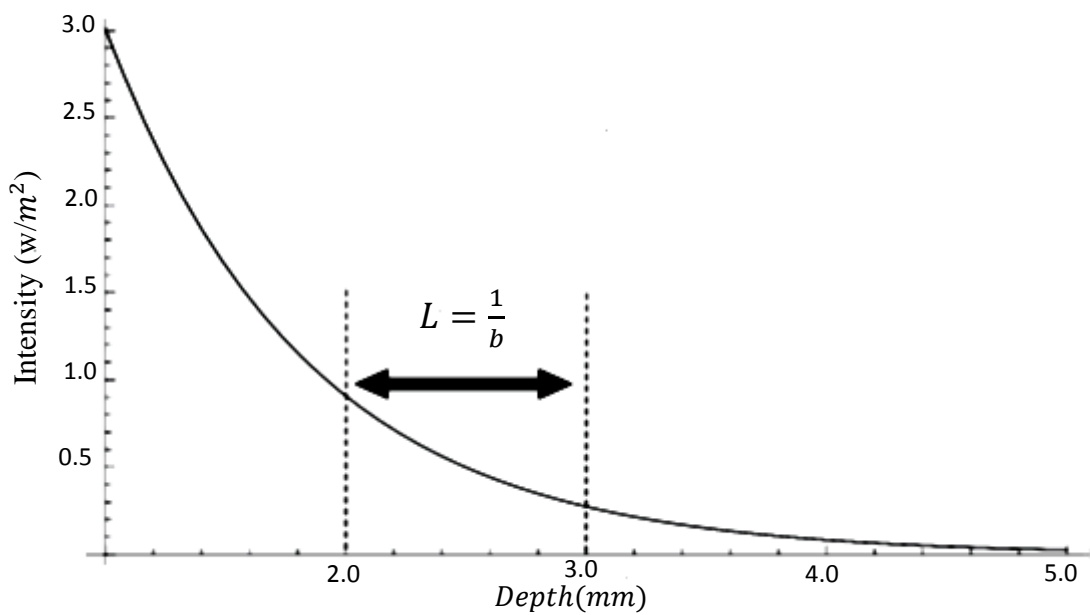


Figure 10: Laser beam reduction as a function of penetration length (radiation) [44]

Beer-Lambert law illustrates that beam intensity ($I(x)$) exponentially decreases with penetration length (x) (Fig.10) as:

$$I = I_0 \cdot e^{-bx} \quad (3.9)$$

Where I_0 is the beam intensity at the surface ($x=0$) and b is the absorption coefficient. The reverse of b is known as the optic absorption length (Fig.10).

$$L = \frac{1}{b} \quad (3.10)$$

The surgical source for laser heating in very short thickness (Δx) is determined by:

$$S_s(x, t) = \frac{I(x) - I(x + \Delta x)}{\Delta x} = -\frac{\partial I(x)}{\partial x} = b \cdot I(x) \quad (3.11)$$

This equation represents that the surgical source is related to the absorbed thermal energy. By substituting Eq.3.11 into Eq.3.9 and considering a term ($H(t)$) with time dependence to model thermal energy with pulse duration (Δt), the surgical source for PBE model is obtained as [47]:

$$S_s(x, t) = (1 - R)bI_0 e^{-bx} [H(t) - H(t - \Delta t)] \quad (3.12)$$

Where R defines the non-denomination Fresnel reflectance and $H(t)$ denotes the Heaviside function with these conditions:

$$H(t) = \begin{cases} 1 & \text{if } t \gg 0 \\ 0 & \text{if } t < 0 \end{cases}$$

Combining Eq.3.3 and Eq.3.12, the final form of parabolic model with interior heat source is:

$$-\frac{\partial^2 T}{\partial x^2}(x, t) + \frac{1}{\alpha} \frac{\partial T}{\partial t}(x, t) = \frac{1}{k} (1 - R)bI_0 e^{-bx} [H(t) - H(t - \Delta t)] + \tau(\delta(t) - \delta(t - \Delta t)) \quad (3.13)$$

Substituting Eq.3.12 into Eq.3.7, the ultimate form of the dominant equation for hyperbolic model is:

$$-\frac{\partial^2 T}{\partial X^2} + \frac{1}{\alpha} \left(\frac{\partial T}{\partial t}(x, t) + \tau \frac{\partial^2 T}{\partial t^2}(x, t) \right) = \frac{1}{k} (1 - R) b I_0 e^{-bx} [H(t) - H(t - \Delta t) + \tau(\delta(t) - \delta(t - \Delta t))] \quad (3.14)$$

Where $\delta(t)$ denotes the Dirac delta function as follow:

$$\delta(t) = \begin{cases} \infty & \text{if } t = 0 \\ 0 & \text{if } t \neq 0 \end{cases}$$

At the tissue surface ($x = 0$), Newton's formula of cooling expresses an equation for convective heat flux as:

$$q(0, t) = h[T_a - T(0, t)] \quad (3.15)$$

Where T_0 and T_a are initial and ambient temperature respectively and h is the ambient convection coefficient.

The corresponding primary condition ($t=0$) for modeling laser heating in human cornea is defined for $\forall x > 0$ as:

$$T(x, 0) = T_0, \quad \frac{\partial T}{\partial t}(x, 0) = 0 \quad (3.16)$$

By substituting Eq.3.15 into the Eq.3.2, the last boundary condition at tissue surface ($x=0$) is obtained for $\forall t > 0$ as:

$$\frac{\partial T}{\partial x}(0, t) = \frac{h}{k} \left(\tau \frac{\partial T}{\partial t}(0, t) + T(0, t) - T_a \right) \quad (3.17)$$

3.3 Numerical Method

3.3.1 Discretizing of PBE Model with Finite Difference Method

According to the Finite Difference Method, the transient form of the bio-heat conduction Eq.3.3 in time step (n+1) is formulated as:

$$\frac{1}{\alpha} \frac{T_i^{n+1} - T_i^n}{(\Delta t)} - \frac{T_{i+1}^{n+1} - 2T_i^{n+1} + T_{i-1}^{n+1}}{(\Delta x)^2} = \frac{1}{k} (1 - R) b I_0 e^{-bx} [H(t) - H(t - \Delta t)] \quad (3.18)$$

This equation is also known as implicit method, where the first term from left to right (transient term) indicates the central difference of $\frac{\partial T}{\partial t}$ of order (Δt) and second term (diffusion term) represents the finite difference for central grid (i) of order $(\Delta x)^2$ at the time step n+1 where Δx is the distance between two adjacent grid points . In this finite difference equation, there are more than one unknown values $(T_{i+1}^{n+1}, T_i^{n+1}$ and $T_{i-1}^{n+1})$ which are illustrated in in Fig.11. As most of these equations are definitely constant, implicit method has a considerably benefit on them. Although this method can be applied in large time steps, these steps have restrictions because the truncation error will be increased in the finite difference equation.

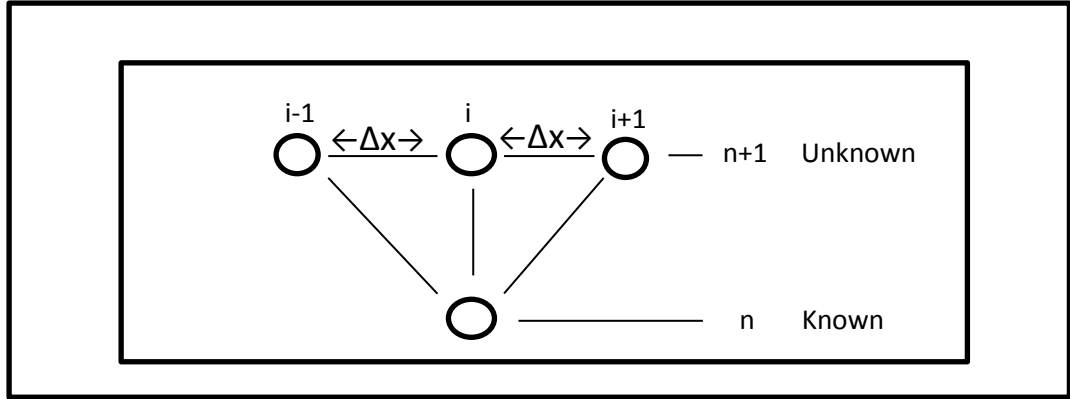


Figure 11: An illustration of the internal nodes for implicit method

3.3.2 Cranks-Nicolson Method

One of the most common applied implicit formulization is Crank-Nicolson method.

This kind of method is definitely stable of orders $[(\Delta t)^2 \text{ and } (\Delta x)^2]$. The first stage

is to estimates $\frac{\partial T}{\partial t}$, $\frac{\partial^2 T}{\partial x^2}$ and $\frac{\partial^2 T}{\partial t^2}$ by using of finite difference method. These

partial derivatives are defined as follow:

$$\frac{\partial T}{\partial t} = \frac{T_i^{n+1} - T_i^n}{(\Delta t)}$$

$$\frac{\partial^2 T}{\partial x^2} = \frac{(T_{i+1}^{n+1} - 2T_i^{n+1} + T_{i-1}^{n+1}) + (T_{i+1}^n - 2T_i^n + T_{i-1}^n)}{2(\Delta x)^2} \quad (3.19)$$

$$\frac{\partial^2 T}{\partial t^2} = \frac{T_i^{n+1} - 2T_i^n + T_i^{n-1}}{(\Delta t)^2}$$

Substituting first and second equations into the Eq.3.18 for internal node and describing diffusion term as the middle level of central differences at the time steps n and n+ 1 result in Crank-Nicolson method as follow:

$$\frac{1}{\alpha} \left(\frac{T_i^{n+1} - T_i^n}{\Delta t} \right) - \frac{1}{2(\Delta x)^2} (T_{i+1}^{n+1} - 2T_i^{n+1} + T_{i-1}^{n+1} + T_{i+1}^n - 2T_i^n + T_{i-1}^n) = \frac{1}{k} (1 - R) b I_0 e^{-bx} [H(t) - H(t - \Delta t)] \quad (3.20)$$

From now on, for decreasing the risk of confusion, the quantities T_i^{n+1} , T_{i-1}^{n+1} and T_{i+1}^{n+1} will be defined as T_P^{n+1} , T_W^{n+1} and T_E^{n+1} respectively and the surgical source will be assumed as a constant value like B. Since it does not change in various time steps.

Multiplying parentheses in their coefficients yields:

$$\begin{aligned} & \frac{-T_E^{n+1}}{2\Delta x^2} + \frac{2T_P^{n+1}}{2\Delta x^2} - \frac{T_W^{n+1}}{2\Delta x^2} - \frac{T_E^n}{2\Delta x^2} + \frac{2T_P^n}{2\Delta x^2} - \frac{T_W^n}{2\Delta x^2} + \frac{T_P^{n+1}}{\alpha\Delta t} - \frac{T_P^n}{\alpha\Delta t} \\ & = B \end{aligned} \quad (3.21)$$

Rearranging equation above leads to:

$$\begin{aligned} T_P^{n+1} \left[\frac{1}{\Delta x^2} + \frac{1}{\alpha\Delta t} \right] &= T_E^{n+1} \left[\frac{1}{2\Delta x^2} \right] + T_W^{n+1} \left[\frac{1}{2\Delta x^2} \right] + T_P^n \left[-\frac{1}{\Delta x^2} + \frac{1}{\alpha\Delta t} \right] + \\ T_E^n \left[\frac{1}{2\Delta x^2} \right] &+ T_W^n \left[\frac{1}{2\Delta x^2} \right] + B \end{aligned} \quad (3.22)$$

Since this thesis tries to solve a numerical instance of corneal tissue according to finite difference method, Eq.3.22 should be setup at each grid point as:

$$A_P T_P^{n+1} = A_E T_E^{n+1} + A_W T_W^{n+1} + S_u \quad (3.23)$$

Where A_P, A_E, A_W and S_u are defined as:

$$A_P = \left[\frac{1}{\Delta x^2} + \frac{1}{\alpha \Delta t} \right]$$

$$A_E = \left[\frac{1}{2\Delta x^2} \right]$$

$$A_W = \left[\frac{1}{2\Delta x^2} \right]$$

$$S_u = T_P^n \left[-\frac{1}{\Delta x^2} + \frac{1}{\alpha \Delta t} \right] + T_E^n \left[\frac{1}{2\Delta x^2} \right] + T_W^n \left[\frac{1}{2\Delta x^2} \right] + B$$

3.3.3 Discretizing of HBE Model with Finite Difference Method

Combining Eqs.3.13 and 3.19 in time steps n and $n+1$ and assuming the surgical source as a constant quantity like c results in:

$$\frac{1}{\alpha} \left[\frac{T_P^{n+1} - T_P^n}{(\Delta t)} + \tau \frac{T_P^{n+1} - 2T_P^n + T_P^{n-1}}{(\Delta t)^2} \right] - \left[\frac{(T_E^{n+1} - 2T_P^{n+1} + T_W^{n+1}) + (T_{i+1}^n - 2T_i^n + T_{i-1}^n)}{2(\Delta x)^2} \right] = C \quad (3.24)$$

Multiplying the parentheses in their coefficients leads to:

$$\frac{-T_E^{n+1}}{2\Delta x^2} + \frac{2T_P^{n+1}}{2\Delta x^2} - \frac{T_W^{n+1}}{2\Delta x^2} - \frac{T_E^n}{2\Delta x^2} + \frac{2T_P^n}{2\Delta x^2} - \frac{T_W^n}{2\Delta x^2} + \frac{T_P^{n+1}}{\alpha \Delta t} - \frac{T_P^n}{\alpha \Delta t} + \frac{\tau T_P^{n+1}}{\alpha \Delta t^2} - \frac{2\tau T_P^n}{\alpha \Delta t^2} + \frac{\tau T_P^{n-1}}{\alpha \Delta t^2} = C \quad (3.25)$$

Rearranging the expressions above results in:

$$T_P^{n+1} \left[\frac{1}{\Delta x^2} + \frac{1}{\alpha \Delta t} + \frac{\tau}{\alpha \Delta t^2} \right] = T_E^{n+1} \left[\frac{1}{2\Delta x^2} \right] + T_W^{n+1} \left[\frac{1}{2\Delta x^2} \right] + T_P^n \left[-\frac{1}{\Delta x^2} + \frac{1}{\alpha \Delta t} + \frac{2\tau}{\alpha \Delta t^2} \right] + T_P^{n-1} \left[\frac{-\tau}{\alpha \Delta t^2} \right] + T_E^n \left[\frac{1}{2\Delta x^2} \right] + T_W^n \left[\frac{1}{2\Delta x^2} \right] + C \quad (3.26)$$

By using Eq.3.23 for equation above, quantities A_P, A_E, A_W and S_u are expressed as:

$$A_P = \left[\frac{1}{\Delta x^2} + \frac{1}{\alpha \Delta t} + \frac{\tau}{\alpha \Delta t^2} \right]$$

$$A_E = \left[\frac{1}{2\Delta x^2} \right]$$

$$A_W = \left[\frac{1}{2\Delta x^2} \right]$$

$$S_u = T_P^n \left[-\frac{1}{\Delta x^2} + \frac{1}{\alpha \Delta t} + \frac{2\tau}{\alpha \Delta t^2} \right] + T_P^{n-1} \left[\frac{-\tau}{\alpha \Delta t^2} \right] + T_E^n \left[\frac{1}{2\Delta x^2} \right] + T_W^n \left[\frac{1}{2\Delta x^2} \right] +$$

C

3.3.4 Discretizing of Boundary Condition

Applying Eq.3.19 for Eq.3.16 which is defined for $x=0$ results in:

$$\frac{T_{i+1}^n - T_{i-1}^n}{2\Delta x} = \frac{h}{k} \left(\tau \frac{T_i^{n+1} - T_i^n}{\Delta t} + T(0, t) - T_a \right) \quad (3.27)$$

In this equation, the quantity T_i^{n+1} is the only unknown one. Therefore, above equation is rearranged in order to find T_i^{n+1} as:

$$\left(\frac{k}{h} \left(\frac{T_{i+1}^n - T_{i-1}^n}{2\Delta x} \right) - (T(0, t) - T_a) \right) = \tau \frac{T_i^{n+1} - T_i^n}{\Delta t} \quad (3.28)$$

Finally, quantity T_i^{n+1} is obtained as:

$$T_i^{n+1} = \frac{\Delta t}{\tau} \left(\frac{k}{h} \frac{T_{i+1}^n - T_{i-1}^n}{2\Delta x} - (T(0, t) - T_a) \right) + T_i^n \quad (3.29)$$

Chapter 4

RESULTS AND DISCUSSIONS

In this Chapter, temperature contributions during L-TKP process for both PBE model and modified PBE model (HBE) has been calculated according to Finite Difference Method for two different initial temperatures 35°C and 40°C. The related code is written in FORTRAN programming language. Subsequently, the results are shown in different graphs and differences between parabolic and hyperbolic models are defined separately. For numerical forecasts, some necessary data about optical and thermal properties of the cornea is required (Table 1).

Table 1: Human cornea properties

Thermal properties			Optical properties	
Diffusivity α [m^2/s]	Conductivity k [$W/m^\circ C$]	Convection h [$W/m^2^\circ C$]	Fresnel Reflectance R	Absorption Coefficient b [m]
1.36×10^{-7}	0.556	20	0.024	2000

During laser heating process, environment temperature is assumed 20°C. The pulse duration of laser light is $\Delta t = 2000\mu s$ which radiates the cornea with intensity of $5 \times 10^8 W/m^2$. The thermal relaxation time is $\tau = 10s$ and laser heating of the cornea takes 2 s.

In Section 4.1, the results of mathematical modeling of the cornea for initial temperature 35°C at 7 various penetration depths 0.01, 0.05, 0.1, 0.3, 0.5, 0.7 and 1 mm which are related to time for both PBE and HBE model have been illustrated. At the end, the behavior of two models has been compared and the benefits of HBE model in comparison with PBE model have been mentioned. In Section 4.2 the results for initial temperature 40°C for both PBE and HBE models at the same penetration depths as Section 4.1 have been shown. The effect of increasing initial temperature on behavior of two models has been discussed.

4.1 Temperature Profiles for $T_0 = 35^\circ\text{C}$

Temperature distribution in various penetration depths of the cornea caused by laser heating in 2 seconds has been shown in the diagrams underneath (Fig.12, Fig.13, Fig.14, Fig.15, Fig.16, Fig.17 and Fig.18)

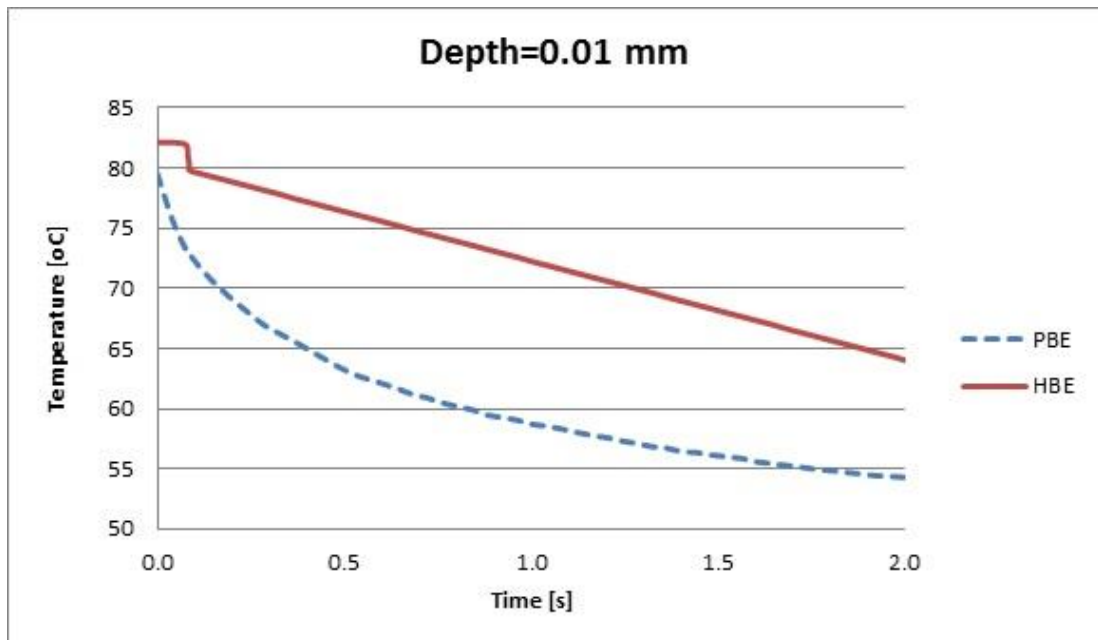


Figure 12: Temperature profile for laser heating of the cornea at $x=0.01\text{mm}$

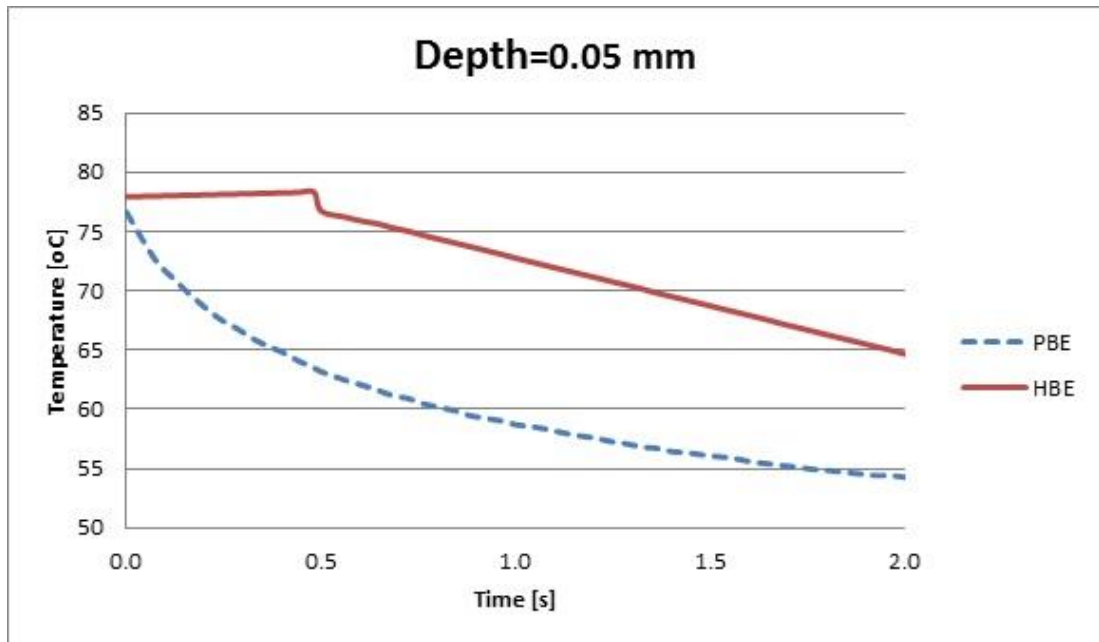


Figure 13: Temperature profile for laser heating of the cornea at $x=0.05$ mm

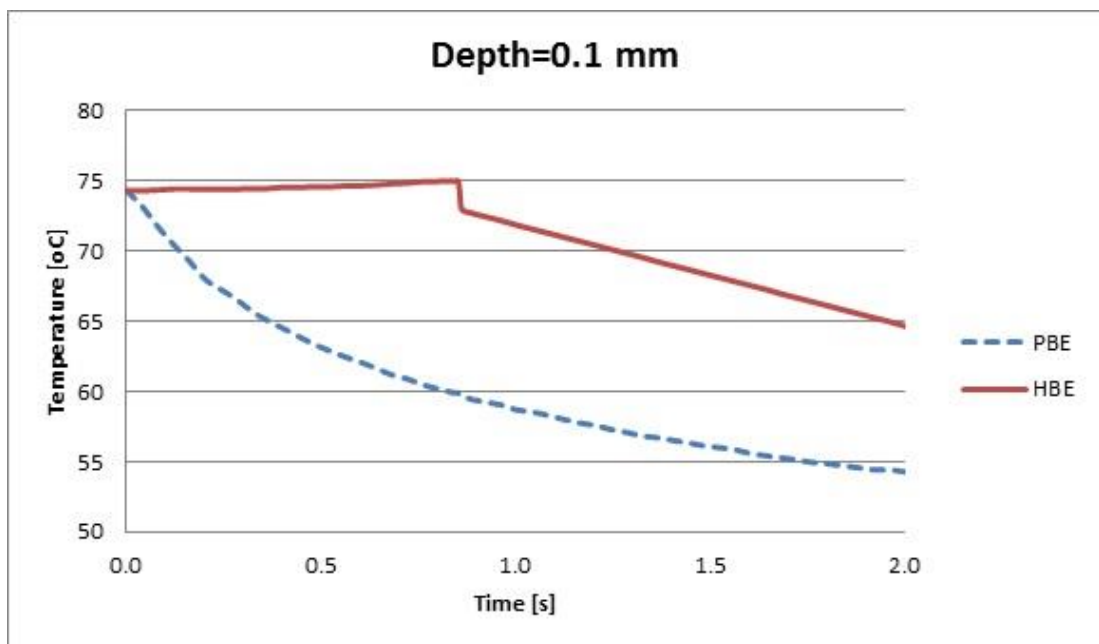


Figure 14: Temperature profile for laser heating of the cornea at $x=0.1$ mm

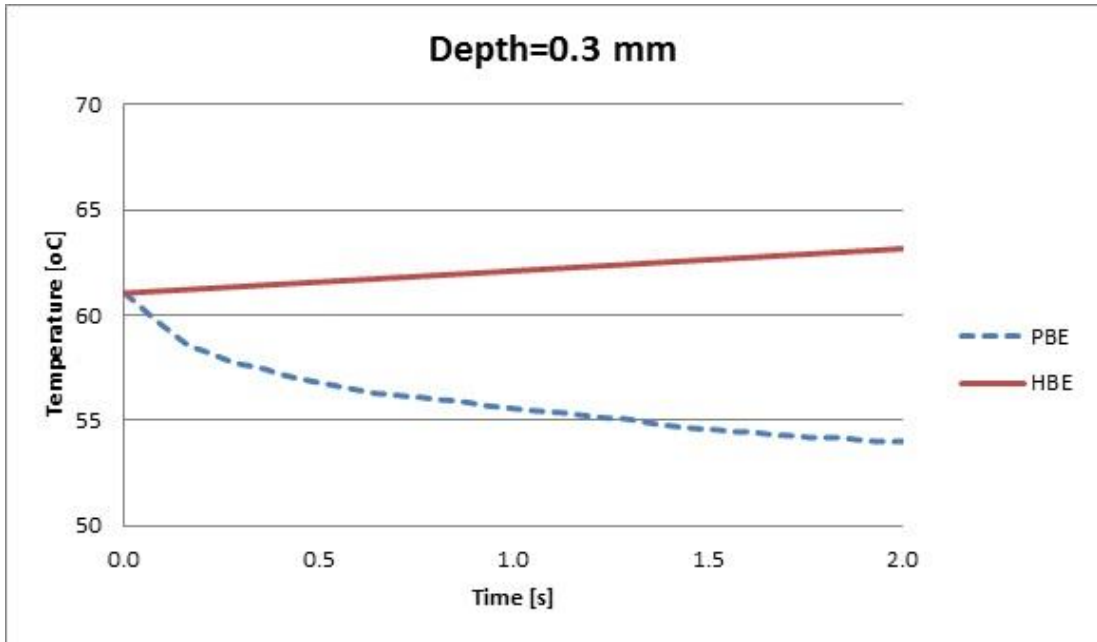


Figure 15: Temperature profile for laser heating of the cornea at $x=0.3$ mm

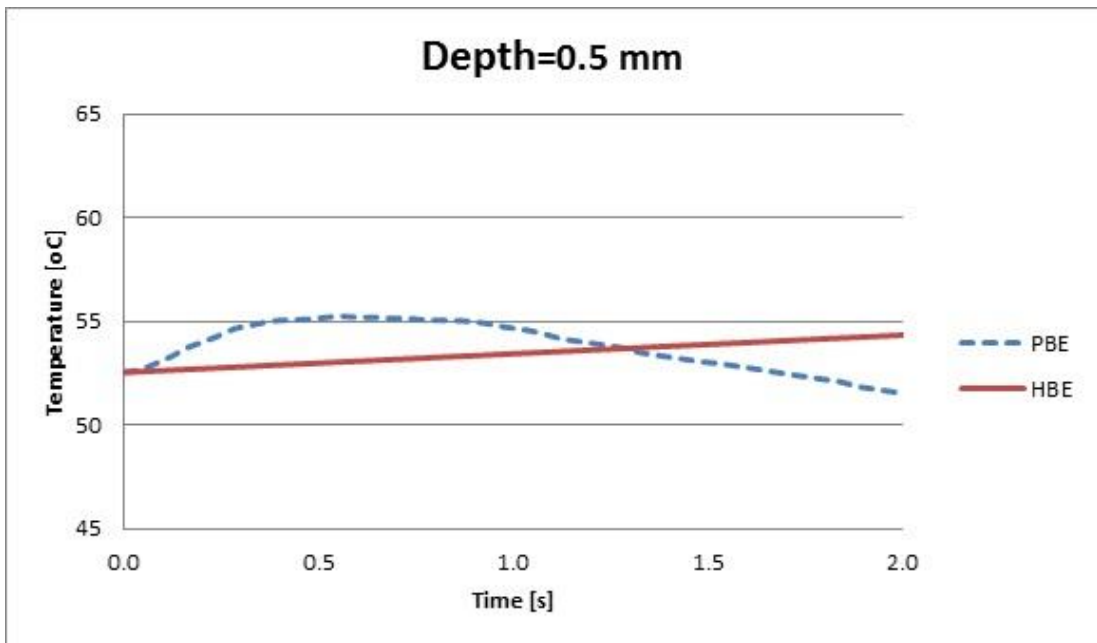


Figure 16: Temperature profile for laser heating of the cornea at $x=0.5$ mm

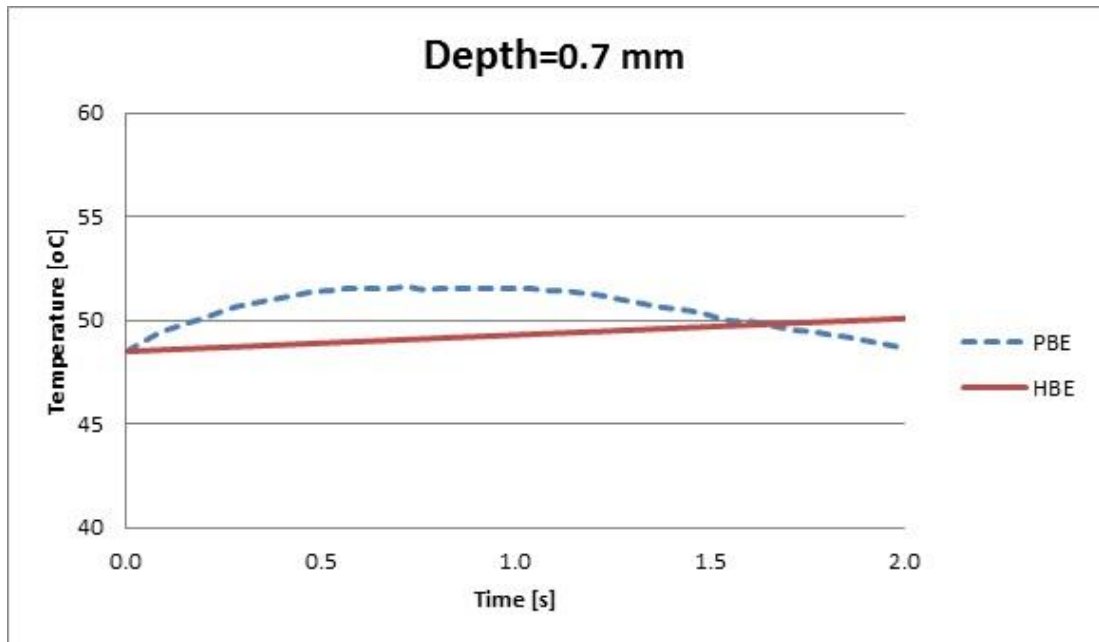


Figure 17: Temperature profile for laser heating of the cornea at x=0.7 mm

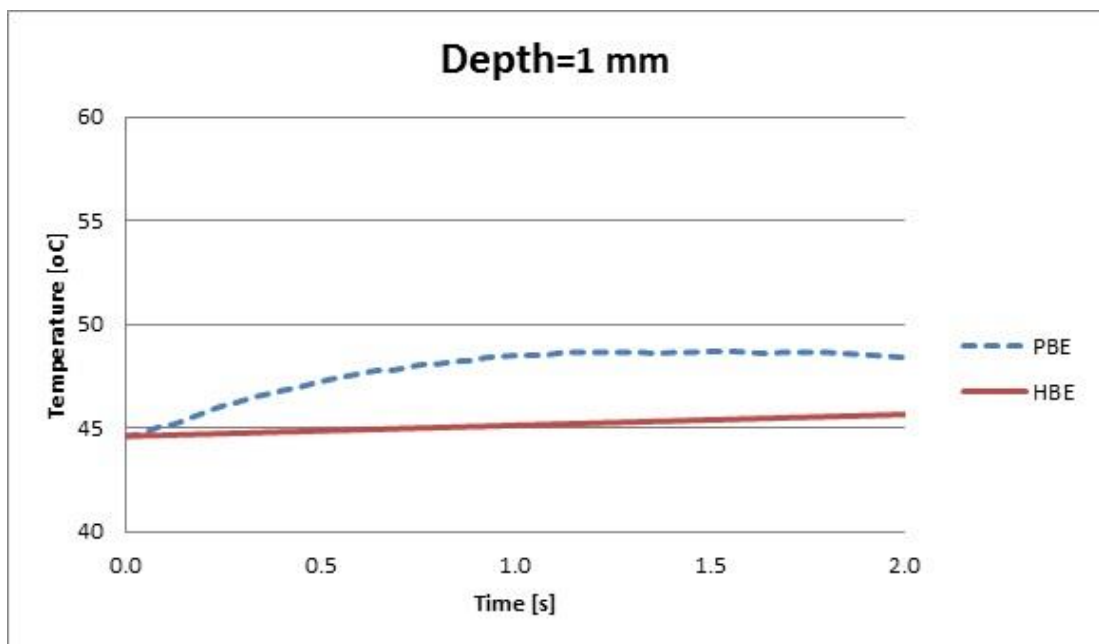


Figure 18: Temperature profile for laser heating of the cornea at x=1 mm

Generally, there are two differences between parabolic and hyperbolic models:

Firstly, for the parabolic model, the highest temperature has been already achieved at the penetration depths 0.01, 0.05 and 0.1 mm and it is continuously declining. The temperature at the next penetration depths 0.3, 0.5, 0.7 and 1 mm has been started at

a lower point in comparison with last ones. Because, as it is mentioned in the Chapter 3, the intensity of laser beam reduces with increasing penetration depth. For the hyperbolic model, it is obvious that the temperature raises in all penetration depths at the beginning of the process. The most difference between the initial temperatures of two models is appeared at the locations near the surface (0.01, 0.05 and 0.1 mm) and this difference has become more and more in each new pulse. Therefore, as it is explained before, the hyperbolic model has an advantage in reaching thermal balance in high temperature in comparison with parabolic model.

Secondly, we can see a delay in the sudden temperature reduction for hyperbolic model at locations 0.01, 0.05 and 0.1 mm which is related to turning off the laser light. Actually, this retardation is relevant to the finite thermal diffusion speed in the hyperbolic model. However, at locations 0.3, 0.5, 0.7 and 1 mm these abrupt reductions of temperature are not seen because they happen beyond the specified time interval. By inserting the numerical amounts for thermal diffusivity (α) and thermal relaxation time (τ) in Eq.3.8, the value of thermal diffusion speed directly obtains as:

$$v = 0.117 \text{ mm/s}$$

This value for finite speed is exactly equal to the known heat propagation speed of the human cornea which illustrates the wave feature of the hyperbolic model.

4.2 Temperature Profiles for $T_0 = 40 \text{ }^\circ\text{C}$

Temperature profiles in various penetration depths of the cornea caused by laser heating in 2 seconds has been presented in the underside figures (Fig.19, Fig.20, Fig.21, Fig.22, Fig.23, Fig.24 and Fig.25).

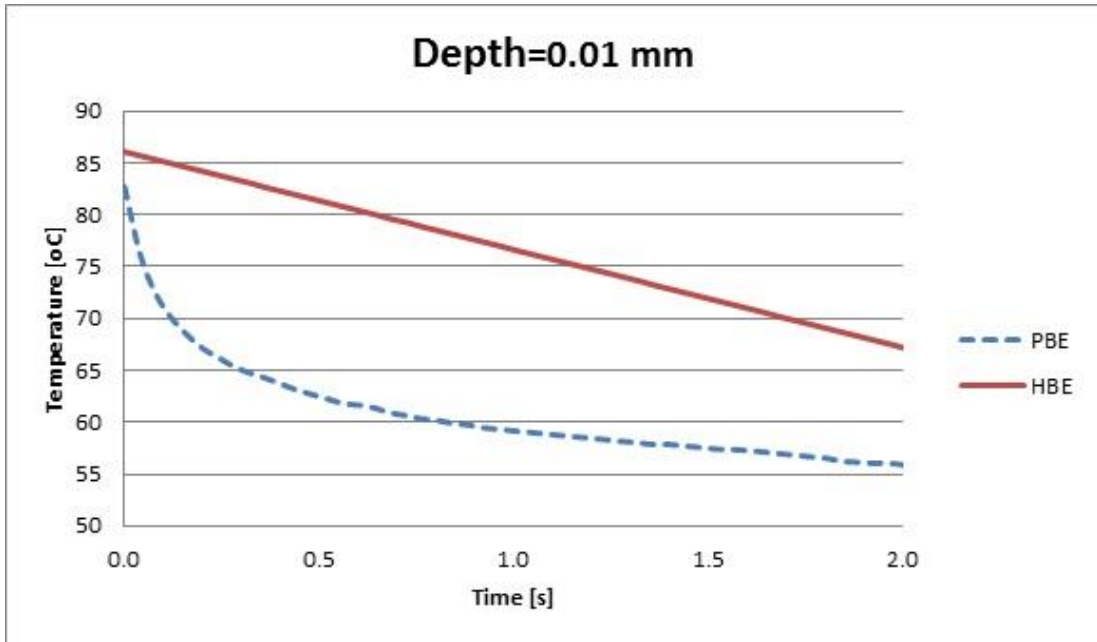


Figure 19: Temperature profile for laser heating of the cornea at $x=0.01$ mm

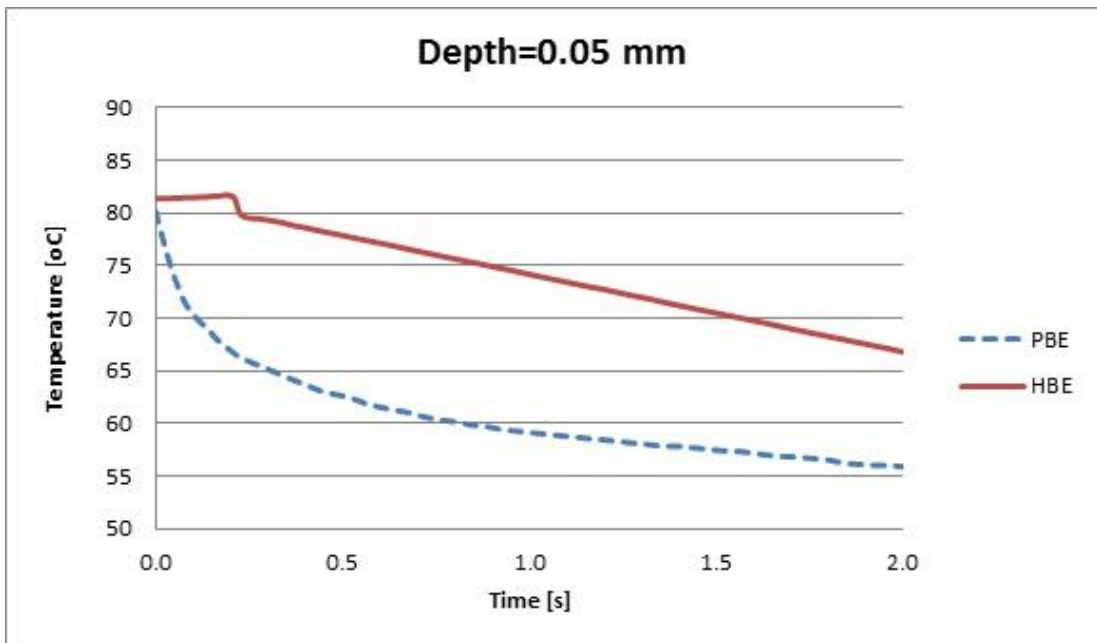


Figure 20: Temperature profile for laser heating of the cornea at $x=0.05$ mm

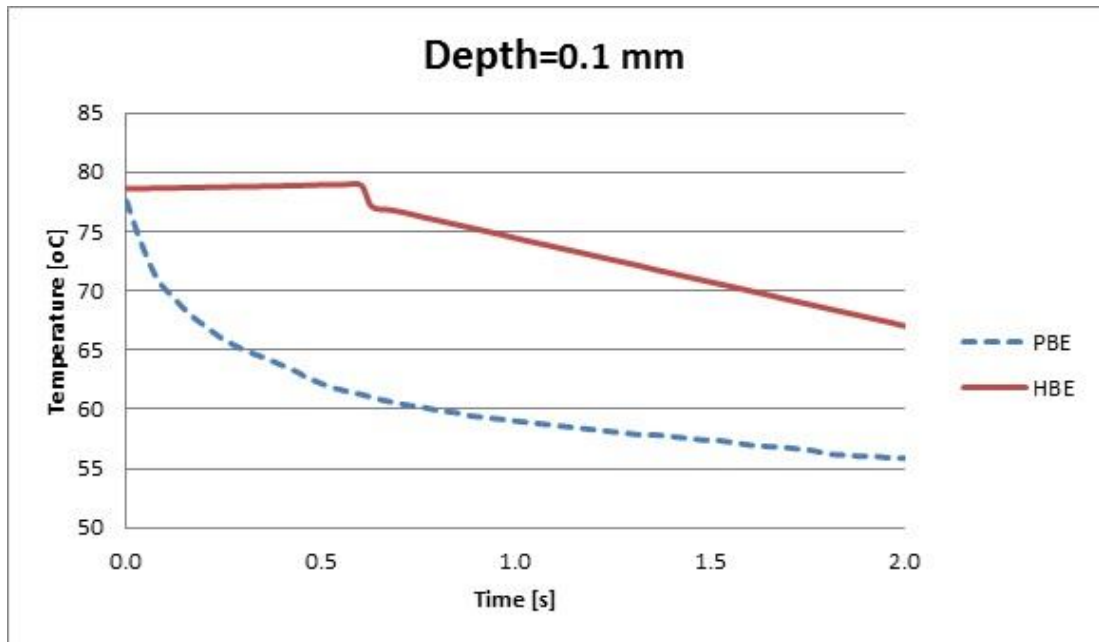


Figure 21: Temperature profile for laser heating of the cornea at $x=0.1$ mm

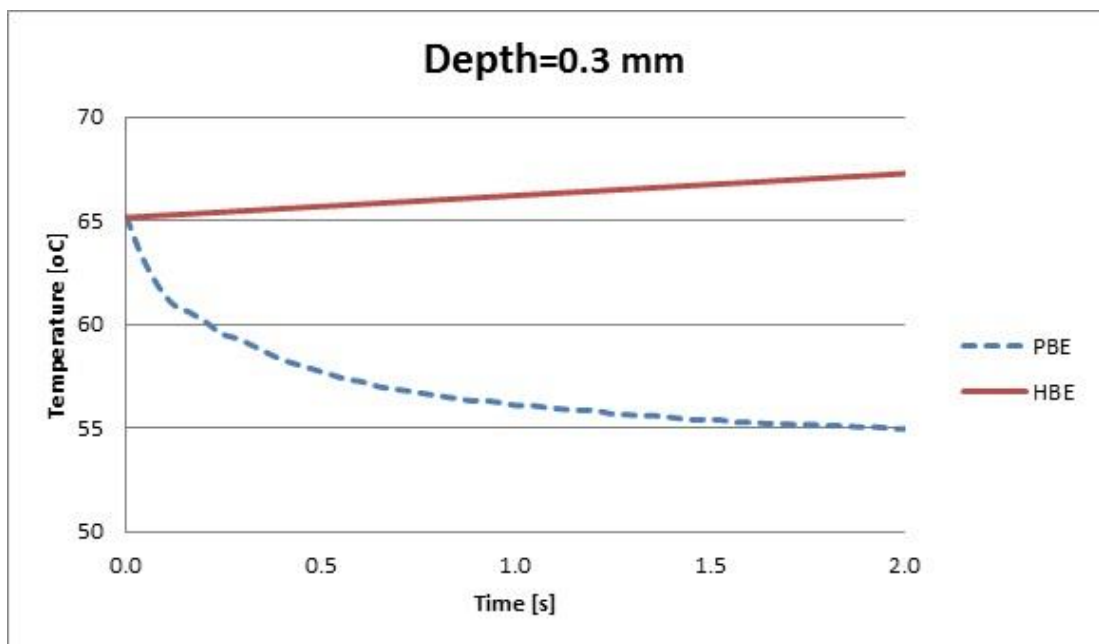


Figure 22: Temperature profile for laser heating of the cornea at $x=0.3$ mm

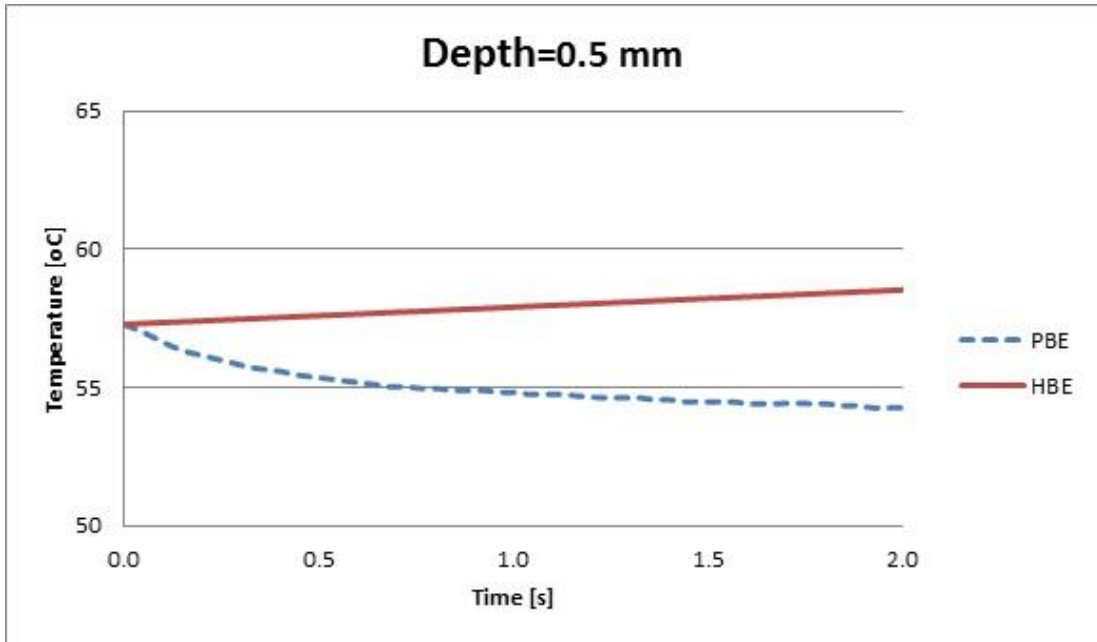


Figure 23: Temperature profile for laser heating of the cornea at $x=0.5$ mm

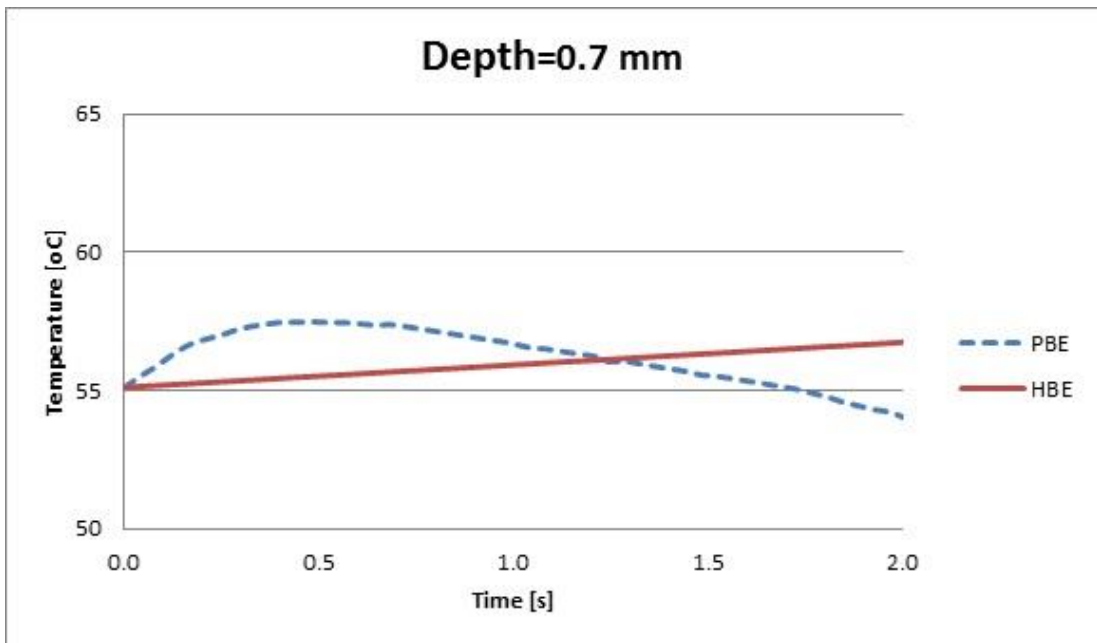


Figure 24: Temperature profile for laser heating of the cornea at $x=0.7$ mm

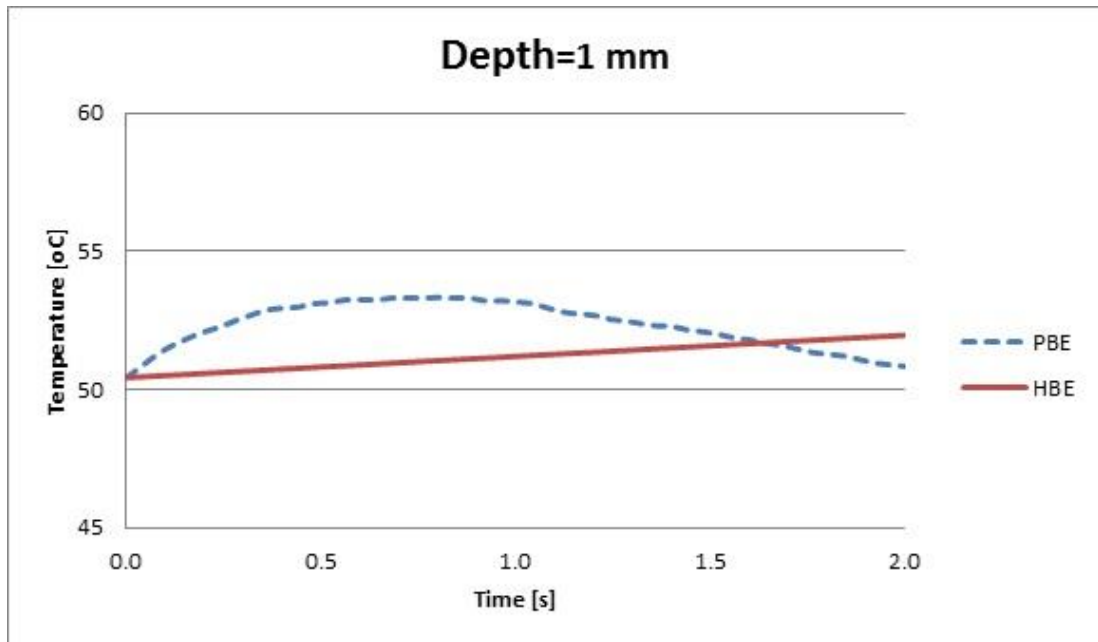


Figure 25: Temperature profile for laser heating of the cornea at $x=1$ mm

Generally, the increasing of initial temperature from $T_0=35^\circ\text{C}$ to $T_0=40^\circ\text{C}$ leads to following expressions:

1) The diagrams illustrate that by increasing the initial temperatures to 40°C all the lines of the diagrams for both parabolic and hyperbolic models are started and finished in higher temperature in comparison with the ones are drawn for initial temperature 35°C .

2) For the parabolic model, at the locations $x=0.01, 0.05, 0.1$ and 0.3 mm the temperature reduction until nearly $t=0.2$ s is more than temperature decline at the same locations in $T_0=35^\circ\text{C}$. For the hyperbolic model, temperature decreasing without initial increasing just take places at penetration depth $x=0.01$ mm. For the aforementioned reasons, the difference between temperatures of two models in $T_0=40^\circ\text{C}$ is more than the difference at the initial temperature 35°C .

3) For parabolic model at penetration depths $x= 0.7$ and 1 mm the temperature drop after initial rising happens earlier in comparison with initial temperature 35°C . The fact is that, increasing initial temperature leads to decreasing the ability of physical system to tolerate the heat of the new laser light.

Chapter 5

CONCLUSION

In this thesis, the basic differences of parabolic and hyperbolic bio-heat equations have been outlined in Chapter 4. These equations were applied to model the heating of human cornea in one-dimension. It is demonstrated that the PBE model could become unsuitable for explaining this phenomenon in which plenty amount of heat fluxes are transmitted to each material in very short time scales. Because heat flux (effect) and the temperature gradient (cause) happen at the same time (t), thermal energy is propagated with infinite speed over the target zone. For aforesaid reasons, this thesis has presented an improved version of PBE model applying hyperbolic bioheat equation (HBE) with finite heat diffusion speed. This model uses thermal relaxation time τ which is necessary for heat propagation after radiation. In this study, Finite Difference Method (FDM) is used for analyzing temperature distribution for both PBE and HBE models in 7 different penetration depths 0.01, 0.05, 0.1, 0.3, 0.5, 0.7 and 1. This analysis has been performed for two various initial temperatures 35°C and 40°C. The differences between two models for both initial temperatures in every depth have been reported and the effect of increasing initial temperature on the behaviors of two models has been investigated. The results show the benefit of HBE model in reaching thermal balance after starting irradiation for both initial temperature in higher heat fluxes and smaller scales of time in comparison with PBE model. Therefore, modeling with regards to HBE approach

has a great impact on the ability of correcting hyperopia by laser which encourages the application of this model for such a process instead of classical model.

REFERENCES

- [1] Albagli, D., "Fundamental Mechanisms of Pulsed Laser Ablation of Biological Tissue," *Laser in Surgery and Medicine*, vol. 4(1), p. 314, August 1987.

- [2] Payrau, P., "Biochemistry and Immunochimistry of the Cornea," *Biochemistry of the Eye*, vol. 20, pp. 1-19, 1996.

- [3] Hugh, D., *The Physiology of the Eye*, London: J. & A. Churchill Ltd, 1949.

- [4] Hugh, D., *The Physiology of the Eye*, fifth edition ed., London: Pergamon press, 1990.

- [5] Bruce, D. M., "Optometric Clinical Practice Guidelines of the Patient with Presbyopia," *Optom*, vol. 21(3), pp. 29-40, 1997.

- [6] Kazuo, T., Brian S. Boxer Wachter, Dimitri T. Azar & Douglas D. Koch, *Hyperopia and Presbyopia (Refractive Surgery)*, London: Informa Healthcare, 2014.

- [7] Chen, J.C., Schmid, K.L. & Brown, B., "The Autonomic Control of Accommodation and Implications for Human Myopia Development," *Ophthalmic & physiological optics*, vol. 23(5), pp. 401-422, 2003.

- [8] Khan-Lim, D., Craig, J.P. & McGhee, C.N., "Defining the Content of Patient Questionnaires: reasons for Seeking Laser in Situ Keratomileusis for Myopia," *J Cat Refract Surg*, vol. 28(5), pp. 788-794, 2002.
- [9] Bailey, M.D., Mitchell, G.L. & Dhaliwal, D.K., "Patient Satisfaction and Visual Symptoms After Laser in Situ Keratomileusis.," *Ophthalmol*, vol. 110(7), pp. 1371-1378, 2003.
- [10] Miller, A.E., McCulley, J.P. & Bowman R.W., "Patient Satisfaction After Lasik for Myopia," *CLAO Journal*, vol. 27(2), pp. 84-88, 2001.
- [11] Soroka, M., Crump, T. & Bennett, A., "Patient Satisfaction with LASIK Surgery in New York State," *Manag Care Interface*, vol. 18(2), pp. 59-62, 2005.
- [12] Koch, D.D., Kohnen, T. & McDonnell, P.J., "Hyperopia Correction by Noncontact Holmium:YAG Laser Thermal Keratoplasty," *United States phase IIA clinical study with a 1-year follow-up*, vol. 103(10), pp. 1525-1535, 1996.
- [13] Mans, F., Borja, D., Parel, J.M., Smiddy, W. & Culbertson, W., "Semianalytical Thermal Model for Subablative Laser Heating of Homogeneous Nonperfused Biological tissue: Application to Laser Thermokeratoplasty," *Jornal Biomedical Optics*, vol. 8(2), pp. 288-297, 2003.
- [14] Ooi, E.H., Ang, W.T. & Ngu, E.Y.K., "A Boundary Element Model of the Human eye Undergoing Laser Thermokeratoplasty," *Computer in Biology and*

Medicine, vol. 38, pp. 727-738, 2008.

- [15] Mainster, M.A., "Ophthalmic Applications of Infrared Lasers-Thermal Considerations," *Investigative Ophthalmology for Visual Science*, vol. 18(4), pp. 414-420, 1979.
- [16] Peppers, Vassiliadis, N.A, Dedrick, K.G., Chang, H., Peabody, R.R. , Rose, H. & Zweng, H.C, "Corneal Damage Threshold for CO2 Laser Irradiation," *Applied Optics*, vol. 8(2), pp. 377-381, 1969.
- [17] Zhou, Z., Ren, Q., Simon, G. & Parel, J.M., "Thermal Modeling of Laser Photo Thermal Keratoplasty (LPTK)," *Ophthalmic Technologies II*, vol. 1644, pp. 61-71, 1992.
- [18] Brinkmann, R., Koop, N., Dröge & Grotehusmann, G.U., "Investigations on Laser Thermokeratoplasty," *Laser Applications in Ophthalmology*, vol. 2079, pp. 120-130, 1994.
- [19] Brinkmann, R., Kampmeier & Grotehusmann, J. U., "Corneal Collagen Denaturation in Laserthermokeratoplasty," *Laser-Tissue Interaction VII*, vol. 2681, pp. 56-62, 1996.
- [20] Mainster, M.A., White, T.J. & Tips, J.H., "Corneal Thermal Response to The CO2 Laser," *Applied Optics*, vol. 9(3), pp. 665-667, 1970.

- [21] Brinkmann, R., Koop, N., Kamm, K., Geerling, G., Kampmeier, J. & Birngruber, R., "Laser Thermokeratoplasty by Means of a Continuously Emitting Laser Diode in the Mid-IR," *Lasers in Ophthalmology IV*, vol. 2930, pp. 66-74, 1996.
- [22] Brinkmann, R., Geerling, G., Kampmeie, J., Koop, N., Radt, B. & Birngruber, R., "Laser Thermokeratoplasty: Analysis of in Vitro Results and Refractive Changes Achieved in a First Clinical Study," *Medical Applications of Lasers in Dermatology, Ophthalmology, Dentistry, and Endoscopy*, vol. 3192, pp. 180-186, 1997.
- [23] Brinkmann, R., Radt, B., Flamm, C., Kampmeie, J., Koop, N. & Birngruber, R., "Influence of Temperature and Time on Thermally Induced Forces in Corneal Collagen and the Effect on Laser Thermokeratoplasty," *Journal of Cataract and Refractive Surgery*, vol. 26(5), pp. 744-754, 2000.
- [24] Zheltov, A.S. & Podol'stev, "Photodestructive Effect of IR Laser Radiation on the Cornea," *Geometrical and Applied Optics*, vol. 102(1), pp. 142-146, 2007.
- [25] Arnab Sarkar, Alamelu, D. & Agarwal, S.K., "Determination of Trace Constituents in Thoria by Laser Induced Breakdown Spectrometry," *Journal of Nuclear Materials*, vol. 385, pp. 158-162, 2009.
- [26] Bohigian, R.K., Shapshay, S.M. & Hybels, R.L., "Management of Rhinophyma with Carbon Dioxide Laser: Lahey Clinic Experience," *Laser Surg Med.*, vol.

8(4), pp. 397-401, 1988.

- [27] Hibst, R. & Kaufmann, R. , "Pulsed Er:YAG and 308 nm UV-Eximer Laser," *Laser in Surgery and Medicine*, vol. 9(2), pp. 132-140, 1989.
- [28] Boris Majaron, Shyam M. Srinivas, L. Huang, J. & Stuart Nelson, "Deep Coagulation of Dermal Collagen with Repetitive Er:YAG Laser Irradiation," *Lasers in Surgery and Medicine*, vol. 26(2), pp. 215–222, 2000.
- [29] Deckelbaum, L.I., "Coronary Laser Angioplasty," *Laser in Surgery and Medicine*, vol. 14(2), pp. 101-110, 1994.
- [30] Izzat, J.A., Albagli, D., Itzkan, I. & Feld, M.S. , "Pulse Laser Ablation of Classified Tissue: Physical Mechanisms and Fundamental Parameters," *Laser-Tissue Interactions SPIE*, vol. 1202, pp. 133-140, 1990.
- [31] Li, Z.Z., Code, J.E. & Van De Merve, W.P., "Er:YAG Laser Ablation of Enamel and Dentin of Human Teeth Determination of Ablation Rates at Various Fluences and Pulse Repetition Rates," *Laser in Surgery and Medicine*, vol. 12(6), pp. 625-630, 1992.
- [32] Hibst, R. & Keller, U., "Experimental Studies of the Application of the Er:YAG Laser on Dental Hard Substances: I: Measurements of the Ablation Rates," *Laser Surg Med*, vol. 9(4), pp. 338-344, 1989.

- [33] Quigley, M.R., Shih, T., Elrifai, A. & Maroon, J.C., "Percutaneous Laser Discectomy with Ho:YAG Laser," *Laser in Surgery and Medicine*, vol. 12(6), pp. 621-624, 1992.
- [34] Chiu, J.C., Clifford, T.J., Greenspan, M., Richley, R.C., Lohman, G. & Sisonm R.B., "Percutaneous Microdecompressive Endoscopic Cervical Endoscopic Microcompressive Thoracic Discectomy with Laser Thermodiskoplasty," *Mt Sinai J Med*, vol. 64(7), pp. 278-820, 2000.
- [35] Choy, D.S., "Percutaneous Laser Disc Decompression (PLDD): Twelve Years' Experience with 752 Procedures in 518 Patients," *Journal of Clinical Laser Medicine and Surgery*, vol. 16(6), pp. 325–331, 1998.
- [36] Johson, D.E., "Use of Holmium: YAG (Ho:YAG) Laser for Treatment of Superficial Bladder Carcinoma," *Laser in Surgery and Medicine*, vol. 14(3), pp. 213-218, 1994.
- [37] Spindel, M.L., Moslem, A., Bhatia, K.S. & Tytle, T., "Comparison of Holmium and Flashlamp Pumped Dye Lasers for Use in Lithotripsy of Biliary Calculi," *Laser in Surgery and Medicine*, vol. 12(6), pp. 482-489, 1992.
- [38] Duffy, S., Davis, M., Sharp, F. & Stamp, G., "Preliminary Observations of Holmium:YAG Laser Tissue Interaction Using Human Uterus," *Laser in Surgery and Mdicine*, vol. 12(2), pp. 147-152, 1992.

- [39] Izzat, J.A , Albagli, D., Itzkan, I. & Feld, M.S., "Pulsed Laser Ablation of Calcified Tissue: Physical Mechanisms and Fundamental Parameters," *Laser Tissue Interactios*, vol. 1202, pp. 133-140, 1990.
- [40] Neumann, A., Sanders, D., Raanan, M. & Deluca, M., "Hyperopic Thermokeratoplasty: Clinical Evaluation," *Journal of Cataract Refract Surgery*, vol. 17(6), pp. 830-838, 1991.
- [41] Trokel, S.L., Srinivasan, R. & Braren, B., "Excimer Laser Surgery of the Cornea," *Am J Ophthalmol*, vol. 96(6), pp. 710-715, 1983.
- [42] Fogle, J.A., Kenyon, K.R. & Stark, W.J., "Damage to Epithelial Basement Membrane by Thermokeratoplasty," *Am J Ophthalmol*, vol. 83(3), pp. 392-401, 1977.
- [43] Brinkmann, R., Radt, B., Flamm, C., Kampmeie, J., Koop, N. & Birngruber, R., "Influence of temperature and time on thermally induced forces in corneal collagen and the effect on laser thermokeratoplasty," *Journal of Cataract Refractive Surgery*, vol. 26(5), pp. 744–754, 2000.
- [44] Pennes, H.H., "Analysis of Tissue and Arterial Blood Temperatures in the Resting Human Forearm," *Journal of Applied Physiology*, vol. 85(1), pp. 5-34, 1998.

- [45] Seffen, K.A. & Lu, T.J., "Non-Fourier Analysis of Skin Biothermomechanics," *International Journal of Heat and Mass Transfer*, vol. 51, pp. 2237-2259, 2008.
- [46] Özisik, M.N. & Tzou, D.T., "On the Wave Theory in Heat Conduction," *Journal of Heat Transfer*, vol. 116(3), pp. 526–535, 2004.
- [47] Manns, F., Borja, D., Parel, J.M., Smiddy, W. & Culbertson, W. ,
"Semianalytical thermal model for subablative laser heating of homogeneous nonperfused biological tissue: Application to laser thermokeratoplasty," *Journal of Biomedical Optics*, vol. 8(2), pp. 288-297, 2003.

APPENDICES

Appendix A: Parabolic Bio-heat Equation

```
PROGRAM TEMPERATURE_DISTRIBUTION

USE VARIABLES

CALL INPUT

CALL GRIDS

!!!!!!!!!!!!!!first time step!!!!!!!!!!!!!!

Call Initialize

CALL Surgical_source

CALL BOUNDRY_COEFFICIENTS

CALL First_time_step

CALL AP_COEFFICIENT

CALL TDMA

CALL UPDATE_TEMP

CALL PRINT_RESULTS

CALL UPDATE_TEMP

DO time_step=dt,Time,Dt

CALL UPDATE_TEMP

CALL Surgical_source

CALL BOUNDRY_COEFFICIENTS

CALL INTERNAL_COEFFICIENTS

CALL AP_COEFFICIENT

CALL TDMA

CALL PRINT_RESULTS

END DO

END PROGRAM TEMPERATURE_DISTRIBUTION

SUBROUTINE INPUT

USE VARIABLES
```

```
N=100.  
L=0.001  
T0=35.  
K=0.556  
alpha=1.3696E-7  
Dt=2.E-3  
Tao=10.  
R=0.024  
E0=5.E8  
b=2000.  
Time=2.  
Ta=20.  
h=20.  
END SUBROUTINE INPUT
```

```
SUBROUTINE GRIDS
```

```
USE VARIABLES
```

```
DX=L/(N-2)
```

```
X(1)=0
```

```
X(2)=(DX/2)
```

```
X(N-1)=L-(DX/2)
```

```
X(N)=L
```

```
DO I=3, N-2
```

```
    X(I)=X(I-1)+DX
```

```
END DO
```

```
DO I=2,N-1
```

```
    DXW(I)=X(I)-X(I-1)
```

```

DXE(I)=X(I+1)-X(I)

END DO

END SUBROUTINE GRIDS

```

```

SUBROUTINE INTERNAL_COEFFICIENTS

```

```

USE VARIABLES

```

```

DO I=3,N-2

```

```

    AW(I)=1./(2.*(DX**2.))

```

```

    AE(I)=1./(2.*(DX**2.))

```

```

    SP(I)=(-1./(alpha*Dt))-(tao/(alpha*(Dt**2.)))

```

```

    Told_term=Told(I)*( (-1./(DX**2.)) + ( 1./(alpha*Dt) ) + ( 2.*tao/(alpha*(Dt**2.)) ) )

```

```

    Told2_term=Told2(I)*( -tao/( alpha*(Dt**2.)) )

```

```

    Told_east_term=Told(I+1)*( 1./(2.*(DX**2.)) )

```

```

    Told_west_term=Told(I-1)*( 1./(2.*(DX**2.)) )

```

```

    SU(I)= Told_term + Told2_term + Told_east_term + Told_west_term + Surg_source(I)

```

```

END DO

```

```

END SUBROUTINE INTERNAL_COEFFICIENTS

```

```

SUBROUTINE BOUNDRY_COEFFICIENTS

```

```

USE VARIABLES

```

```

!SP(2)=-AW(2)

```

```

!SP(N-1)=-AE(N-1)

```

```

!SU(2)=AW(2)*TA

```

```

!AW(2)=0

```

```

!SU(N-1)=AE(N-1)*TB

```

```

!AE(N-1)=0

```

```

SP(2)=-1.

```

```

SP(N-1)=-1.
!Textra=2.*Told(2)-Told(3)
Textra=((-h*Dx/K)*(T0-Ta))+ Told(2)
SU(2)=Told(2)+(Dt/2.)*( K*( (Told(3)-Textra)/(2.*Dx) )/h ) -(T0-Ta )
SU(N-1)=T0
AW(2)=0.
AE(2)=0.
AE(N-1)=0.
AW(N-1)=0.
END SUBROUTINE BOUNDRY_COEFFICIENTS

```

```

SUBROUTINE AP_COEFFICIENT
USE VARIABLES
DO I=2,N-1
AP(I)=AW(I)+AE(I)-SP(I)
END DO
END SUBROUTINE AP_COEFFICIENT

```

```

SUBROUTINE TDMA
USE VARIABLES
DO I=3,N-1
MULT=AW(I)/AP(I-1)
AP(I)=AP(I)-MULT*AE(I-1)
SU(I)=SU(I)-MULT*SU(I-1)
END DO
T(N-1)=SU(N-1)/AP(N-1)
DO I=N-2,2,-1

```

```
T(I)=(SU(I)-(AE(I)*T(I+1)))/AP(I)
```

```
END DO
```

```
END SUBROUTINE TDMA
```

```
SUBROUTINE PRINT_RESULTS
```

```
USE VARIABLES
```

```
OPEN (3,FILE='TEMPERATURE.TXT')
```

```
WRITE(3,*) 'I      X(I)      T(I)'
```

```
DO I=2,N-1
```

```
WRITE(3,*) I,X(I),T(I), Dt
```

```
!10 FORMAT(I2,10X,F10.6,8X,F11.6,8X,F11.6)
```

```
END DO
```

```
END SUBROUTINE PRINT_RESULTS
```

```
SUBROUTINE UPDATE_TEMP
```

```
USE VARIABLES
```

```
DO I=2,N-1
```

```
Told2(I)=Told(I)
```

```
Told(I)=T(I)
```

```
time_step=time_step+Dt
```

```
END DO
```

```
END SUBROUTINE UPDATE_TEMP
```

```
SUBROUTINE Surgical_source
```

```
USE VARIABLES
```

```
call Heaviside
```

```
call Dirac
```

```

Surg_term=(1.-R)*b*E0/k

DO I=2,N-1

Surg_source(I)=Surg_term* exp(-b*X(I))*( Ht-HtDt+tao*(Delta_t-Delta_Dt) )

END DO

END SUBROUTINE Surgical_source

```

```

SUBROUTINE Heaviside

USE VARIABLES

if(time_step.lt.0)then

    Ht=0.

else if (time_step.eq.0)then

    Ht=0.5

else

    Ht=1.

end if

if(time_step.lt.Dt)then

    HtDt=0.

else if (time_step.eq.Dt)then

    HtDt=0.5

else

    HtDt=1.

end if

END SUBROUTINE Heaviside

```

```

SUBROUTINE Dirac

USE VARIABLES

```



```

if(time_step<tao.and.-tao<time_step)then
    Delta_t=1./(2.*tao)
else
    Delta_t=0.
end if

if((time_step-Dt)<tao.and.-tao<(time_step-Dt))then
    Delta_Dt=1./(2.*tao)
else
    Delta_Dt=0.
end if

END SUBROUTINE Dirac

SUBROUTINE First_time_step
USE VARIABLES
DO I=2,N-1
    AW(I)=1./(2.*(DX**2.))
    AE(I)=1./(2.*(DX**2.))
    SP(I)=(-1./(alpha*Dt)-(tao/(alpha*(Dt**2.))) + ( tao/(alpha*(Dt**2.)) )
    Told_term=Told(I)*( (-1./(DX**2.)) + ( 1./(alpha*Dt) ) + ( 2.*tao/(alpha*(Dt**2.)) ) )
    Told2_term=(-tao*2.*Told(I))/(alpha*Dt**2.)
    Told_east_term=Told(I+1)*( 1/(2.*(DX**2.)) )
    Told_west_term=Told(I-1)*( 1/(2.*(DX**2.)) )
    SU(I)= Told_term + Told2_term + Told_east_term + Told_west_term + Surg_source(I)
END DO
END SUBROUTINE First_time_step

SUBROUTINE Initialize

```

```
USE VARIABLES
```

```
DO I=2,N-1
```

```
T(I)=T0
```

```
Told(I)=T0
```

```
END DO
```

```
END SUBROUTINE Initialize
```

Appendix B: Hyperbolic Bioheat Equation

PROGRAM TEMPERATURE_DISTRIBUTION

USE VARIABLES

CALL INPUT

CALL GRIDS

!!!!!!!!!!!!!!first time step!!!!!!!!!!!!!!

Call Initialize

CALL Surgical_source

CALL BOUNDRY_COEFFICIENTS

CALL First_time_step

CALL AP_COEFFICIENT

CALL TDMA

CALL UPDATE_TEMP

CALL PRINT_RESULTS

CALL UPDATE_TEMP

DO time_step=dt,Time,Dt

CALL UPDATE_TEMP

CALL Surgical_source

CALL BOUNDRY_COEFFICIENTS

CALL INTERNAL_COEFFICIENTS

CALL AP_COEFFICIENT

CALL TDMA

CALL PRINT_RESULTS

END DO

END PROGRAM TEMPERATURE_DISTRIBUTION

SUBROUTINE INPUT

USE VARIABLES

N=100.

L=0.001

T0=35.

K=0.556

alpha=1.3696E-7

Dt=2.E-3

Tao=10.

R=0.024

E0=5.E8

b=2000.

Time=2.

Ta=0.

h=20.

END SUBROUTINE INPUT

SUBROUTINE GRIDS

USE VARIABLES

$DX=L/(N-2)$

$X(1)=0$

$X(2)=(DX/2)$

$X(N-1)=L-(DX/2)$

$X(N)=L$

DO I=3, N-2

$X(I)=X(I-1)+DX$

END DO

DO I=2,N-1

$DXW(I)=X(I)-X(I-1)$

```

DXE(I)=X(I+1)-X(I)

END DO

END SUBROUTINE GRIDS

```

```

SUBROUTINE INTERNAL_COEFFICIENTS

```

```

USE VARIABLES

```

```

DO I=3,N-2

```

```

    AW(I)=1./(2.*(DX**2.))

```

```

    AE(I)=1./(2.*(DX**2.))

```

```

    SP(I)=(-1./(alpha*Dt))-(tao/(alpha*(Dt**2.)))

```

```

    Told_term=Told(I)*( (-1./(DX**2.)) + ( 1./(alpha*Dt) ) + ( 2.*tao/(alpha*(Dt**2.)) ) )

```

```

    Told2_term=Told2(I)*( -tao/( alpha*(Dt**2.)) )

```

```

    Told_east_term=Told(I+1)*( 1./(2.*(DX**2.)) )

```

```

    Told_west_term=Told(I-1)*( 1./(2.*(DX**2.)) )

```

```

    SU(I)= Told_term + Told2_term + Told_east_term + Told_west_term + Surg_source(I)

```

```

END DO

```

```

END SUBROUTINE INTERNAL_COEFFICIENTS

```

```

SUBROUTINE BOUNDRY_COEFFICIENTS

```

```

USE VARIABLES

```

```

!SP(2)=-AW(2)

```

```

!SP(N-1)=-AE(N-1)

```

```

!SU(2)=AW(2)*TA

```

```

!AW(2)=0

```

```

!SU(N-1)=AE(N-1)*TB

```

```

!AE(N-1)=0

```

```

SP(2)=-1.

```

```

SP(N-1)=-1.
!Textra=2.*Told(2)-Told(3)
Textra=((-h*Dx/K)*(T0-Ta))+ Told(2)
SU(2)=Told(2)+(Dt/2.)*( K*( (Told(3)-Textra)/(2.*Dx) )/h ) -(T0-Ta )
SU(N-1)=T0
AW(2)=0.
AE(2)=0.
AE(N-1)=0.
AW(N-1)=0.
END SUBROUTINE BOUNDRY_COEFFICIENTS

```

```

SUBROUTINE AP_COEFFICIENT
USE VARIABLES
DO I=2,N-1
AP(I)=AW(I)+AE(I)-SP(I)
END DO
END SUBROUTINE AP_COEFFICIENT

```

```

SUBROUTINE TDMA
USE VARIABLES
DO I=3,N-1
MULT=AW(I)/AP(I-1)
AP(I)=AP(I)-MULT*AE(I-1)
SU(I)=SU(I)-MULT*SU(I-1)
END DO
T(N-1)=SU(N-1)/AP(N-1)
DO I=N-2,2,-1

```

```
T(I)=(SU(I)-(AE(I)*T(I+1)))/AP(I)
```

```
END DO
```

```
END SUBROUTINE TDMA
```

```
SUBROUTINE PRINT_RESULTS
```

```
USE VARIABLES
```

```
OPEN (3,FILE='TEMPERATURE.TXT')
```

```
WRITE(3,*) 'I      X(I)      T(I)'
```

```
DO I=2,N-1
```

```
WRITE(3,*) I,X(I),T(I), Dt
```

```
!10 FORMAT(I2,10X,F10.6,8X,F11.6,8X,F11.6)
```

```
END DO
```

```
END SUBROUTINE PRINT_RESULTS
```

```
SUBROUTINE UPDATE_TEMP
```

```
USE VARIABLES
```

```
DO I=2,N-1
```

```
Told2(I)=Told(I)
```

```
Told(I)=T(I)
```

```
time_step=time_step+Dt
```

```
END DO
```

```
END SUBROUTINE UPDATE_TEMP
```

```
SUBROUTINE Surgical_source
```

```
USE VARIABLES
```

```
call Heaviside
```

```
call Dirac
```

```

Surg_term=(1.-R)*b*E0/k
DO I=2,N-1
Surg_source(I)=Surg_term* exp(-b*X(I))*( Ht-HtDt+tao*(Delta_t-Delta_Dt) )
END DO
END SUBROUTINE Surgical_source

```

```

SUBROUTINE Heaviside
USE VARIABLES
  if(time_step.lt.0)then
    Ht=0.
  else if (time_step.eq.0)then
    Ht=0.5
  else
    Ht=1.
  end if
  if(time_step.lt.Dt)then
    HtDt=0.
  else if (time_step.eq.Dt)then
    HtDt=0.5
  else
    HtDt=1.
  end if
END SUBROUTINE Heaviside

```

```

SUBROUTINE Dirac
USE VARIABLES
  if(time_step<tao.and.-tao<time_step)then

```



```

        Delta_t=1./(2.*tao)
else
        Delta_t=0.
end if

if((time_step-Dt)<tao.and.-tao<(time_step-Dt))then

        Delta_Dt=1./(2.*tao)
else
        Delta_Dt=0.
end if

END SUBROUTINE Dirac

SUBROUTINE First_time_step
USE VARIABLES
DO I=2,N-1
        AW(I)=1./(2.*(DX**2.))
        AE(I)=1./(2.*(DX**2.))
        SP(I)=(-1./(alpha*Dt)-(tao/(alpha*(Dt**2.))) + ( tao/(alpha*(Dt**2.)) )
        Told_term=Told(I)*( (-1./(DX**2.)) + ( 1./(alpha*Dt) ) + ( 2.*tao/(alpha*(Dt**2.)) ) )
        Told2_term=(-tao*2.*Told(I))/(alpha*Dt**2.)
        Told_east_term=Told(I+1)*( 1/(2.*(DX**2.)) )
        Told_west_term=Told(I-1)*( 1/(2.*(DX**2.)) )
        SU(I)= Told_term + Told2_term + Told_east_term + Told_west_term + Surg_source(I)
END DO

END SUBROUTINE First_time_step

SUBROUTINE Initialize
USE VARIABLES

```

```
DO I=2,N-1  
T(I)=T0  
Told(I)=T0  
END DO  
END SUBROUTINE Initialize
```